

Chapter 2

Electrical Logging

2.1 The Foundation of Electrical Resistivity

The resistivity of a substance is its ability to impede the flow of electrical currents. The ability of a formation to conduct electricity is directly related to the amount of water in the formation. This is true since the formation grains (matrix) have negligible conductivity (high resistivity). By understanding bed resistivity, it is possible to determine the “water saturation” of a formation and hence its hydrocarbon saturation. Formation resistivity can also be related to the porosity of the formation.

2.1.1 Resistivity

Electrical resistivity of any material is related to the resistance by the following equation:

$$R = r \times a/L,$$

where

a area in square meters of rock material exposed to the current flow

L length of the material in meters

r electrical resistance in ohms

R electrical resistivity expressed in ohm-meters.

Formation resistivities usually range from 0.2 to 1,000 Ω -m. Resistivities higher than 1,000 Ω -m are uncommon in permeable formations. Most formations are made up of rocks which when dry will not conduct electrical currents. Current flow in a formation is through interstitial water made conductive by salts in solution. These salts dissociate into positively charged sodium cations and negatively charged

anions. Ions move under the influence of an electrical field, carrying an electrical current through the solution. Greater salt concentration lowers the formation water resistivity,

The resistivity of the water is:

$$\text{Resistivity} = (R_w \times L)/a$$

We measured R_w with a test meter. L is the length of the cube, which is 1 m. The area is 1 m by 1 m. Solving the equation:

$$\text{Resistivity} = (R_w \times 1)/(1 \times 1) = R_w$$

In this case, the resistivity of the water is the same as its measured resistance.

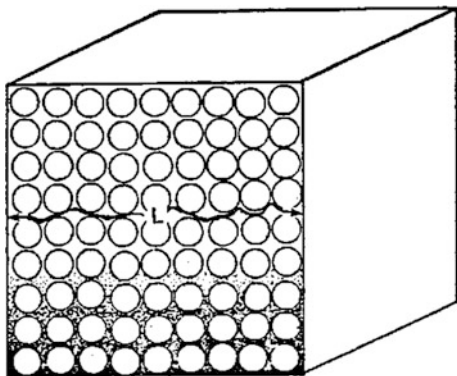
Now let us take one cubic meter of formation rock and insert it into the cube filled with water. What happens to some of the water? Yes, it spills over as the rock occupies the volume. Looking at Fig. 2.1, we now have a cube with formation rock that is 100 % saturated with water. The resistivity of this cube is called R_o .

When the cube had only water, it was simple to see that an ion could travel from one side of the cube to the other in a straight path. The length of this travel was 1 m. Now that we have added the formation rock to the cube, the ion must find a meandering path, greater than 1 m, around the rock grains to go from one side to the other.

The length of this ion cannot be measured. The best that can be done is simply to estimate it based on the texture of the rock, the cementation, and the amount of pore space available. We will consider this in more detail later in the text.

To complete our cubic reservoir, let us take some water out and replace it with oil. Because the oil is lighter than the water it will float on top. We still have the length L ; the porosity factor; and the resistivity of the water to consider. The only difference is that we no longer have 100 % water. We took some out and replaced it with oil (Fig. 2.1). If we took out 40 % of the water, then we would have 60 % left

Fig. 2.1 Model of a rock bearing liquid



in the cube. This 60 % is called the water saturation, or S_w . Now the total resistivity of the cube is:

$$\text{Resistivity} = (R_w \times L) / (\emptyset \times S_w)$$

In reality, the water saturation is what we want to know. If we can measure the total resistivity, the porosity, the water resistance, and estimate the length L , then we can solve the equation for S_w . It then follows that the amount of hydrocarbons is $1 - S_w$.

It should be mentioned here that the resistivity of the water is not only a function of salinity but also of temperature. The higher the temperature is, the lower is the resistivity at a given salinity, so that water resistivity will vary according to temperature.

The following equation shows the general method for calculating formation temperature so that it can be applied toward adjusting the resistivity of the formation itself.

$$T_f = T_o + (G_g \times D_f) / 100,$$

where

- T_f the formation temperature
- T_o the mean annual surface temperature
- G_g the geothermal gradient expressed in °F per 100 ft
- D_f the formation depth in feet.

Surface temperature is defined as the average annual temperature at some depth, typically from 70 to 100 ft below the surface of the earth, where seasonal temperature variations average out. This surface temperature may vary according to location.

For the purpose of log analysis, however, surface temperatures 5–10° higher than these produce more satisfactory results. Formation temperature may also be determined from the chart in Fig. 3.2.

Because mud filtrate invades the formation, it is important for us to know what the mud filtrate resistivity is. The mud filtrate resistivity is measured at the surface with a cup-type device, and that resistivity is adjusted for temperature at the formation depth.

$$R_2 = R_1 \times \frac{T_1 + 6.77}{T_2 + 6.77}$$

This is the ARPS formula for determining resistivity at formation temperature. T_1 is the mean surface temperature expressed in °T. T_2 is the formation temperature in °T. R_1 is the resistivity at T_1 , and R_2 is the resistivity at T_2 .

In a formation containing oil or gas, both of which are insulators, resistivity is a function of the formation factor F , the water resistivity R_w , and the water saturation

S_w . The **saturation** of a fluid in a formation is the ratio of the volume occupied by the fluid to the total pore volume, i.e., it is the fraction of the porosity occupied by that particular fluid. If the fluid is formation water, then its saturation S_w , is:

$$S_w = V_w/V_p$$

where, V_w is volume occupied by formation water, and V_p if volume of pores. If there no other fluids present, then $V_w = V_p$, and $S_w = 1.0$. If some hydrocarbon (V_h) is present, then $V_h = V_p - V_w$, and now:

$$S_w = (V_p - V_h)/V_p = V_w/V_p$$

N.B. Saturation is a dimensionless quantity being a ratio. It is expressed either as a decimal ($0 < S_w < 1.0$) or as a percentage ($0 \% < S_w < 100 \%$).

2.1.2 Archie Formula

As discussed earlier, the unknown factor is the length of the path of the ionic current. The length of this path is 1 m for R_w and greater than one for R_o , which is the true resistivity of the formation of porosity totally saturated with water of resistivity R_w . This unknown quantity is called the formation resistivity factor or simply F . This factor is defined as:

$$F = R_o/R_w$$

For a constant porosity, the ratio of R_o to R_w remains nearly constant for all values of R_w below 1 Ω -m. Experiments show that in more resistive waters, the value of F is reduced as R_w rises. This phenomenon is due to a greater influence of the surface conductance of the grains in fresh waters.

The value of R_o , should be calculated, rather than picked from the log. Finding a clean zone that is 100 % saturated with water is a difficult task. This places us in a difficult position because we must know the value of the formation factor.

Archie experimentally determined that the formation factor could be determined from three factors, i.e., porosity (ϕ), cementation (m) and rock texture (a). So the above equation can be expressed as:

$$F = \frac{R_o}{R_w} = \frac{\alpha}{\phi^m},$$

where a is a coefficient varies from 0.6 to 2.0 depending on the texture of rock, and m is the cementation or tortuosity factor. It varies between 1 and 3 according to the type of sediment, the pore-shape, the type of porosity, and its distribution.

If hydrocarbon is presented in pores, the resistivity of the formation is not R_o , but R_t , and the water saturation is not equals to 100 %. Through a large number of laboratory measurements, Archie determined experimentally that the water saturation of a clean formation can be expressed in terms of its true resistivity.

$$S_w^n = R_o/R_t,$$

where n is the saturation exponent. It is determined empirically, and lies between 1.2 and 2.2.

Combining the above two equations we can get the so-called Archie equation:

$$S_w = \sqrt[n]{\frac{\alpha R_w}{R_t \phi^m}}$$

Through extensive use of this relationship, the following values have been used with great success:

$$F = 0.81/\phi^2 \quad \text{in sands rocks}$$

$$F = 1/\phi^2 \quad \text{in carbonate rocks}$$

These two formulas are similar to the Humble formula developed from an intensive study of sandstone samples in the 1950s.

2.1.3 *Electrical Properties of Rocks and Brines*

There are two general types of conduction of interest to us: electrolytic and metallic. In **electrolytic** conduction, the mechanism is dependent upon the presence of dissolved salts in a liquid such as water. Examples of electrolytic conduction are provided with metal, which are not covered here.

The following Table 2.1 illustrates the resistivity of some typical materials. Notice the range of resistivity variation for salt water, which depends on concentration of NaCl. Typical rock materials are in essence insulators. The fact that reservoir rocks have any detectable conductivity is usually the result of the presence of electrolytic conductors in the pore space. In some cases, the resistivity of a rock may result from the presence of metal, graphite, metal sulfides, or clays. The table shows that the resistivity of formations of interest may range from 0.5 to 103 Ω m, nearly four orders of magnitude.

The conductivity of sedimentary rocks is primarily of electrolytic origin. It is the result of the presence of water and combination of water and hydrocarbons in the pore space in a continuous phase. The actual conductivity will depend on the

Table 2.1 Typical resistivity value of rocks, minerals, and fluids

Medium	Resistivity (Ω m)	Medium	Resistivity (Ω m)
Clay	1–200	White mica	4×10^{11}
Clay (mud rock)	5–60	Feldspar	4×10^{11}
Shale	10–100	Petroleum	10^9 – 10^{16}
Unconsolidated sand	2–50	Calcite	5×10^3 – 5×10^{12}
Tight sand	20–1000	Graphite	10^{-6} – 3×10^{-4}
Oil-sand	2–1000	Madnetite	10^{-4} – 6×10^{-3}
Shell-limestone	20–2000	Pyrite	10^{-4}
Limestone	50–10,000	Copper pyrite	10^{-3}
Dolomite	50–10,000	Oil and gas	
Basalt	60 – 10^5	Gas	
Granite	60 – 10^5	Brine (15 °C, 2 kppm)	3.4
Anhydrite	10^4 – 10^6	Fresh water	
Quartz	10^{12} – 10^{14}		

resistivity of the water in the pores and the quantity of water present. To a lesser extent, it will depend on the lithology of the rock matrix, its clay content, and its texture (grain size, and the distribution of pores, clay, and conductive minerals). Finally, the conductivity of a sedimentary formation will depend strongly on temperature.

Figure 2.2 graphically presents the resistivity of saltwater (NaCl) solutions as a function of electrolyte concentration and temperature. According to the preceding analysis, the resistivity is expected to depend inversely on the charge carrier concentration.

2.1.4 Borehole Environment

Before concluding this chapter, let us examine the schematic representation of a well bore (Fig. 2.3a, b). R_{mc} is the mud cake resistivity, h_{mc} is the thickness of the mud cake, D_i is the diameter of invasion, h is the bed thickness, D_h is the hole diameter, R_{xo} is the resistivity of the flushed portion of the invaded zone, R_{mf} is the resistivity of the mud filtrate, and S_{xo} is the flushed zone water saturation.

In the uninvaded zone, R_t is the true virgin formation resistivity. R_w is the formation water resistivity, and S_w is the water saturation of the undisturbed formation. Water saturation in the undisturbed or uninvaded zone is the parameter we are most interested in. Its determination allows the log analyst to estimate the amount of hydrocarbons present in a given formation. This information, along with porosity and a permeability estimate, can be used to predict the well's ultimate production.

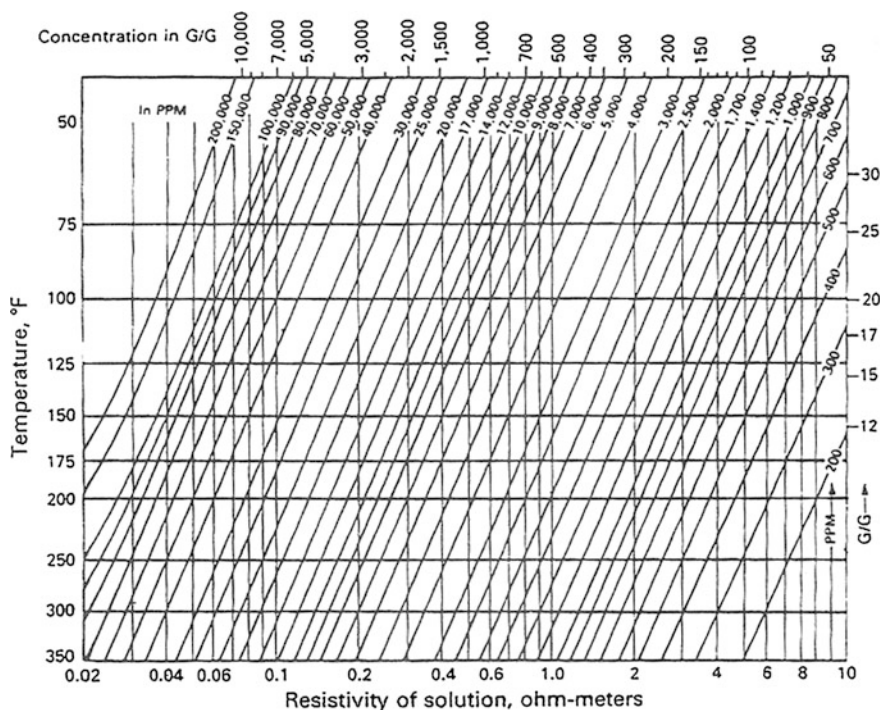


Fig. 2.2 A nomogram for determining the resistivity of an NaCl solution as a function of the NaCl concentration and temperature (from Schlumberger)

2.1.5 Conclusions

It is not important to fully understand each concept presented in this chapter. The purpose is to acquaint you with the basic terms and relationships of analysis. Everything presented here will be covered in great detail in chapters to follow.

2.2 Spontaneous Potential Logging

The spontaneous potential (or SP) curve is a recording of naturally occurring earth potentials between a moveable electrode in the borehole and a fixed surface electrode. Such potentials are in no way induced by the passive measuring equipment. For this reason, SPs are also referred to as “self potentials.” The SP is generally recorded in the left-hand track of the log. The SP is used to:

- Detect permeable beds.
- Locate their boundaries and permit correlation of such beds.

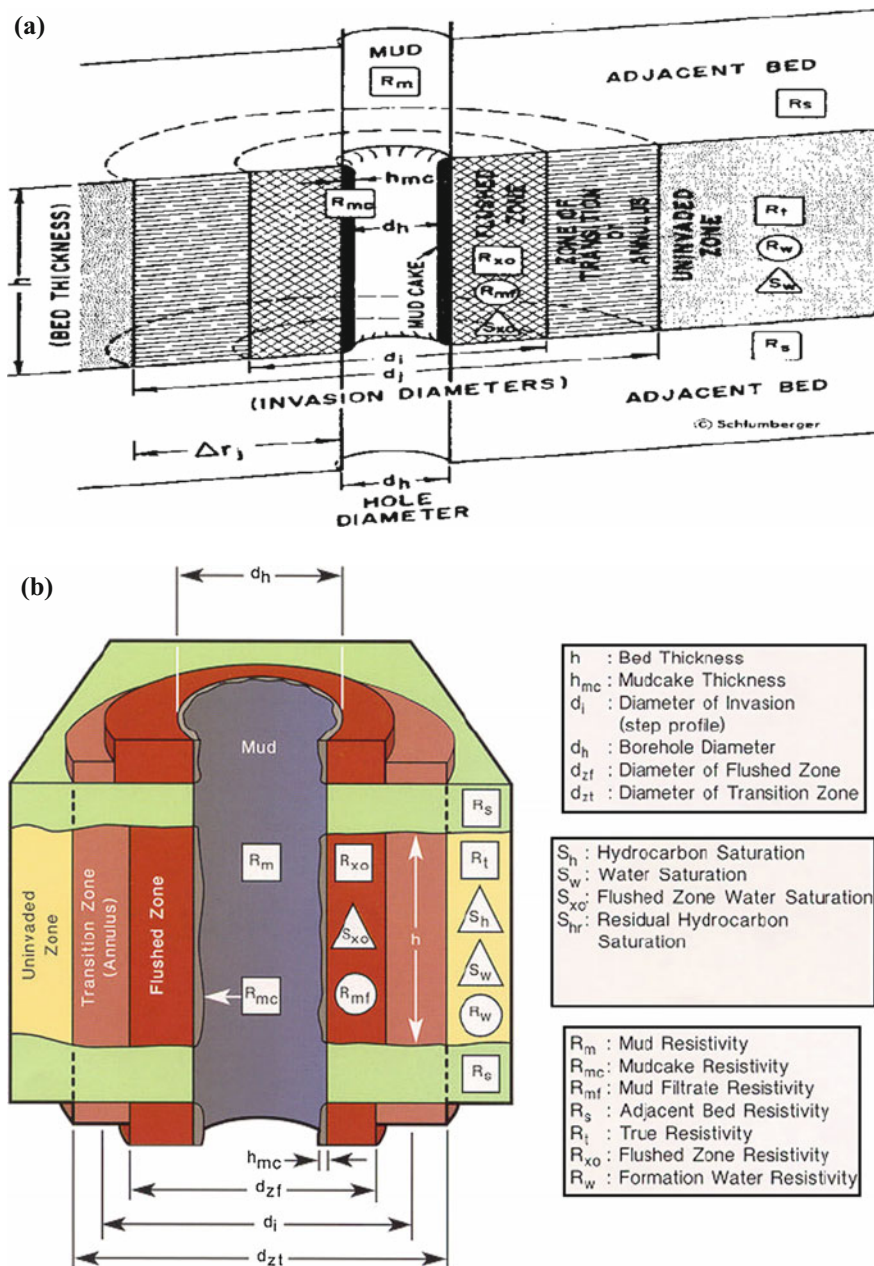


Fig. 2.3 a Environment around borehole, b Environment around borehole

- Determine values of formation water resistivity (R_w).
- Give quantitative indications of bed shaliness.

The readings of the SP in shale are usually fairly constant and tend to follow a straight line on the log, called the shale base line. In permeable formations, the SP curves show excursions from the shale base line. In thick beds it tends to reach an essentially constant deflection defining a sand line. The SP may deflect either to the left (negative) or to the right (positive) of the shale base line, depending on the relative salinities of the formation water and of the mud filtrate. Figure 2.4 illustrates the typical SP response in shale, sand, and limestone.

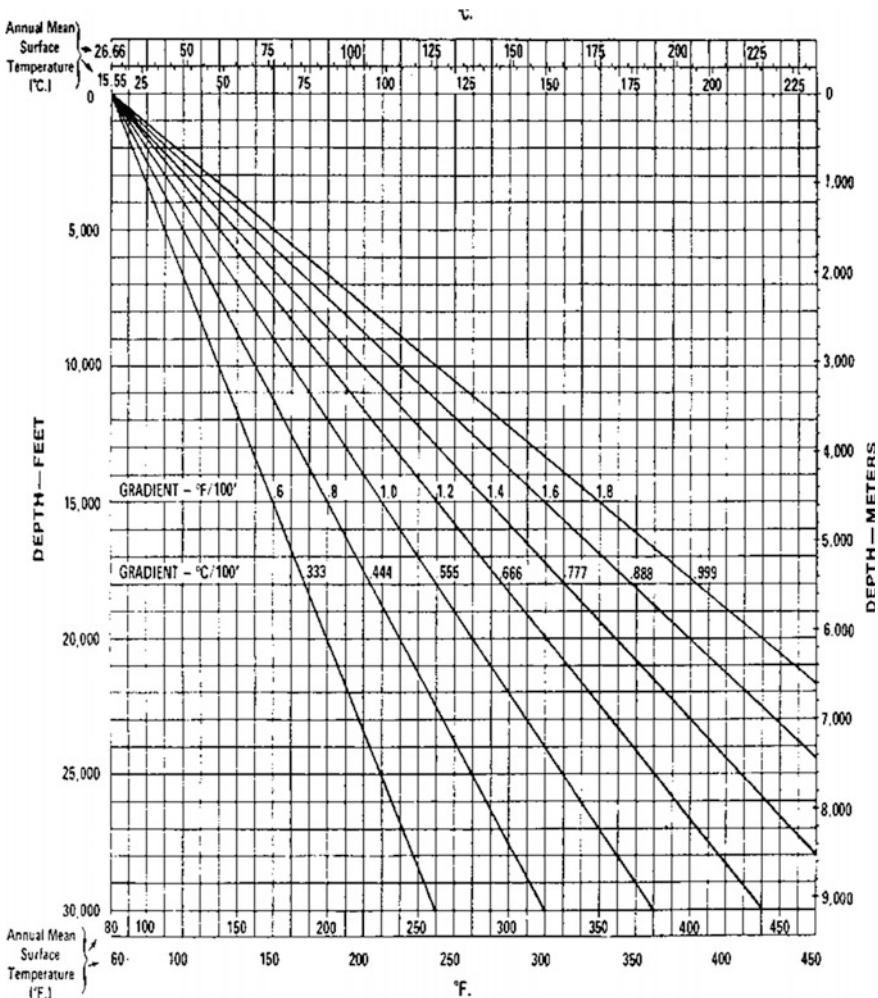


Fig. 2.4 Formation temperature-depth relationship (Courtesy of Gearhart)

2.2.1 The SP Log

Schlumberger discovered this phenomenon in 1928. An electrical potential difference exists, spontaneously, between an electrode in the borehole, and a remote reference electrode on surface. This potential varies from formation to formation, usually within the range of a few tens or hundreds of millivolts (mV). In Fig. 2.5, an electrode A, located at the end of an insulated cable C, is moved up or down the mud-filled borehole. The insulated conductor is connected to one terminal of a recording galvanometer; the other terminal of the galvanometer is connected to a potentiometer circuit P, and then to electrode B, usually placed in the mud pit or in a mud-filled hole dug for this purpose. Electrode B is called the SP ground.

The boreholes in which the SP is recorded are usually filled with water-based mud. The recording galvanometer measures all the differences of potential appearing between electrodes A and B. The deflections on the SP log correspond to phenomena occurring at the contacts between the mud and the different beds, and at the contacts between the beds themselves. These phenomena produce an electric current, which uses the mud as its return path. In doing so, it creates in the mud, by ohmic effect, potential differences which can be measured.

The position of the shale base line on the log recording has no useful meaning for interpretation purposes. SP scale sensitivity is chosen and the shale base line is

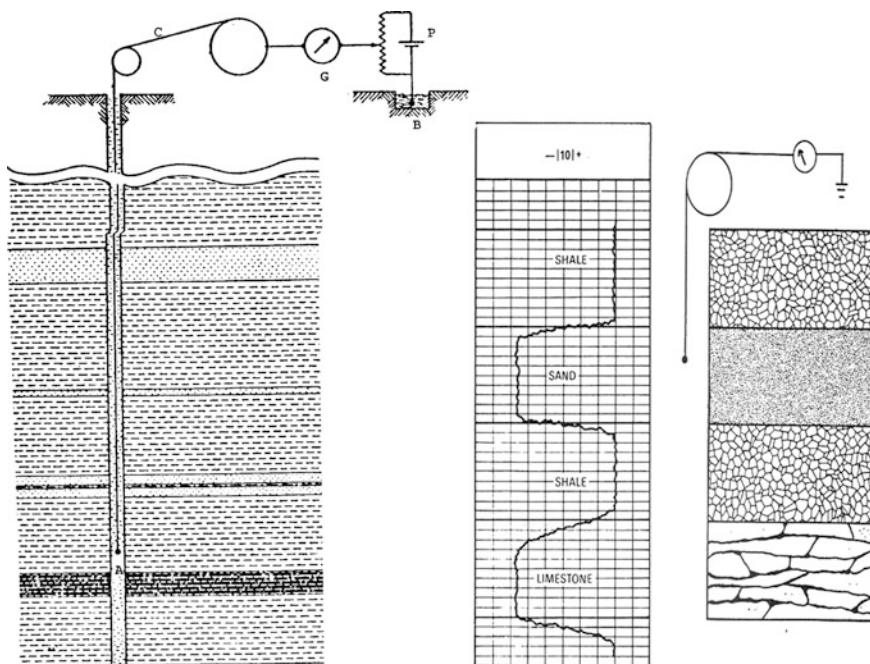


Fig. 2.5 Spontaneous potential

positioned by the logging engineer so that the SP curve deflections remain in the SP track.

The SP cannot be recorded in holes filled with nonconductive muds because such muds do not provide electrical continuity between SP electrodes and formation. Normal SP deflections occur only in porous, permeable beds. The SP log, although indicating permeability, cannot be used to quantify either permeability or porosity.

SP deflections are due to earth currents which develop an electromotive or electrical force in the mud column. These SP currents are generated by two sources called electrochemical and electrokinetic.

Greater significance is often attached to each variation in the SP curve, so the presence of spurious potentials, or potentials induced by outside sources, on the log is undesirable. If present and bothersome, proper steps by the logging engineer should be taken to remove them. Some spurious potentials have no effect on the magnitude of SP deflections. The electrodes are chosen to be stable insofar as their contact potential with the mud is concerned. In practice, lead electrodes are used. A constant difference of potential may normally appear between the surface and down hole electrodes in the absence of any SP current. This difference of potential is not recorded on the SP log; it is counterbalanced by means of the surface potentiometer circuit used to set the shale base line. Accordingly, the potential of the downhole electrode is measured on the SP log with reference to an arbitrary constant. However, variations in potential (that is, the deflections on the SP log) do not depend on the arbitrary constant.

2.2.2 Electrochemical Component of the SP

Consider a permeable formation with thick shale beds above and below. Assume that the two electrolytes present, mud filtrate, and interstitial formation water, contains sodium chloride (NaCl) only. Because of the layered clay structure and the charges on the layers, shales are permeable to the Na^+ cations but impervious to the Cl^- anions. Only the Na^+ cations (positive charges) are able to move through the shale from the more concentrated to the less concentrated NaCl solution. This movement of charged ions is an electric current, and the force causing them to move constitutes a potential across the shale.

The curved arrow in the upper half of Fig. 2.6 shows the direction of current flow corresponding to the passage of Na^+ ions through the adjacent shale from the more saline formation water in the bed to the less saline mud.

Since shales pass only the cations, shales resemble ion-selective membranes, and the potential across the shale is therefore called the membrane potential.

Another component of the electrochemical potential is produced at the edge of the invaded zone, where the mud filtrate and formation water are in direct contact. Here Na^+ and Cl^- ions can diffuse (move) from either solution to the other. Since Cl^- ions have a greater mobility than Na^+ ions, the net result of this ion diffusion is a flow of negative charges (Cl^- ions) from the more concentrated to the less

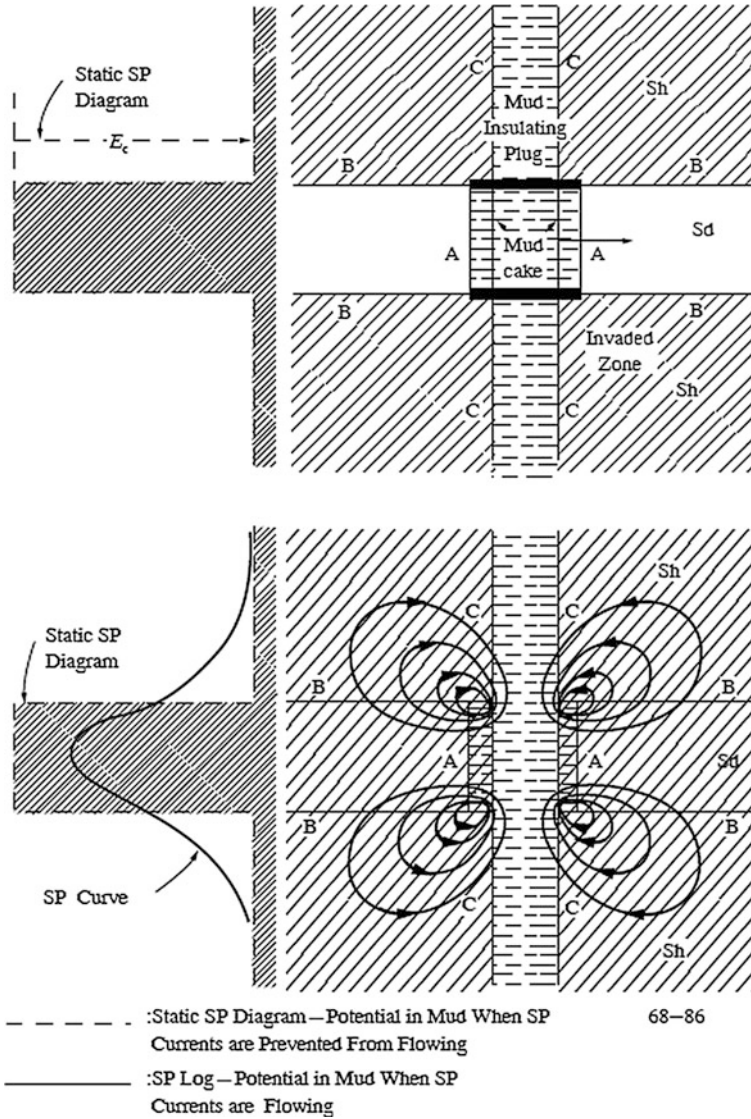


Fig. 2.6 Schematic representation of potential and current distribution in and around a permeable bed

concentrated solution. This is equivalent to a conventional current flow in the opposite direction, indicated by the straight Arrow A in the upper half of Fig. 2.6. The current flowing across the junction between solutions of different salinity is produced by an electromagnetic force (emf) called liquid-junction potential (as shown in Fig. 2.7). The magnitude of the liquid-junction potential is only about one-fifth the membrane potential.

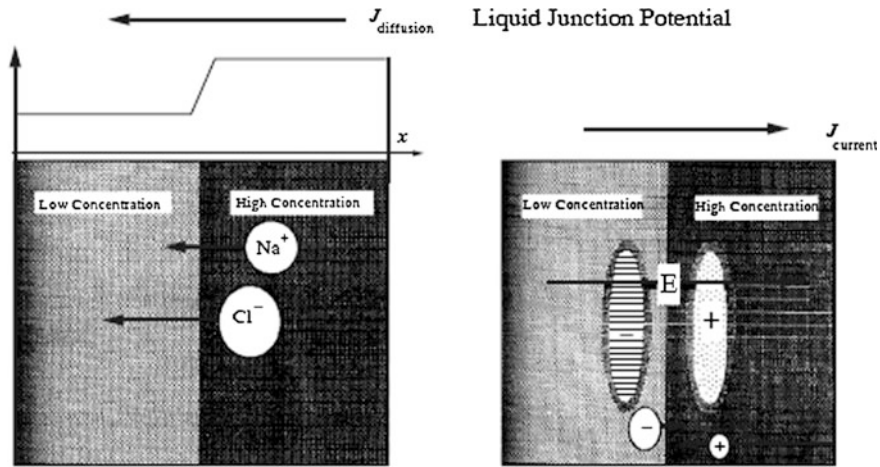


Fig. 2.7 Schematic representation of the mechanism responsible for the generation of the liquid-junction potential. A concentration gradient results in diffusion. The mobility difference between Na^+ and Cl^- causes a charge separation

If the permeable formation is not shaly, the total electrochemical emf, E_c , corresponding to these two phenomena, is equal to:

$$E_c = -K \log \frac{a_w}{a_{mf}},$$

where a_w and a_{mf} are the chemical activities of the two solutions (formation water and mud filtrate) at formation temperature; K is a coefficient proportional to the absolute temperature, and, for NaCl formation water and mud filtrate, is equal to 71 at 25 °C (77 °F). The chemical activity of a solution is roughly proportional to its salt content (i.e., to its conductivity). If the solutions contain substantial amounts of salts other than NaCl, the value of K at 77 °F may differ from 71.

If the permeable formation contains some shale or dispersed clay, the total electrochemical emf and, hence, the SP deflections will be reduced since the clay in the permeable formation produces an electrochemical membrane of opposite polarity to that of the adjacent shale bed.

2.2.3 Spontaneous Potential (SP) Tool

The spontaneous potential (SP) log is a record of the naturally occurring potentials in the wellbore as a function of depth. The SP log involves a single moving electrode in the borehole and a reference electrode, usually located at the surface in

the mud pit or some other suitable location. The recording is a relative measurement of the DC voltage in the borehole with no zero being recorded. Readings opposite shales are relatively constant and are referred to as “the shale baseline.” Opposite permeable formations the SP curve typically shows excursions to the left (negative polarity) or to the right, depending upon the salinity of the drilling mud and formation waters (Fig. 2.8). The position of the shale base line has no real significance. The logging engineer sets the position and sensitivity on the log so that deflections opposite permeable beds stay within the limits of track 1 (on the log). Typically, the shale base line is set two chart divisions (where ten divisions make the total width of the track) from the right edge of the SP track. The variations of the measured SP indicate there are currents flowing within the wellbore. These currents are primarily of an electrochemical nature.

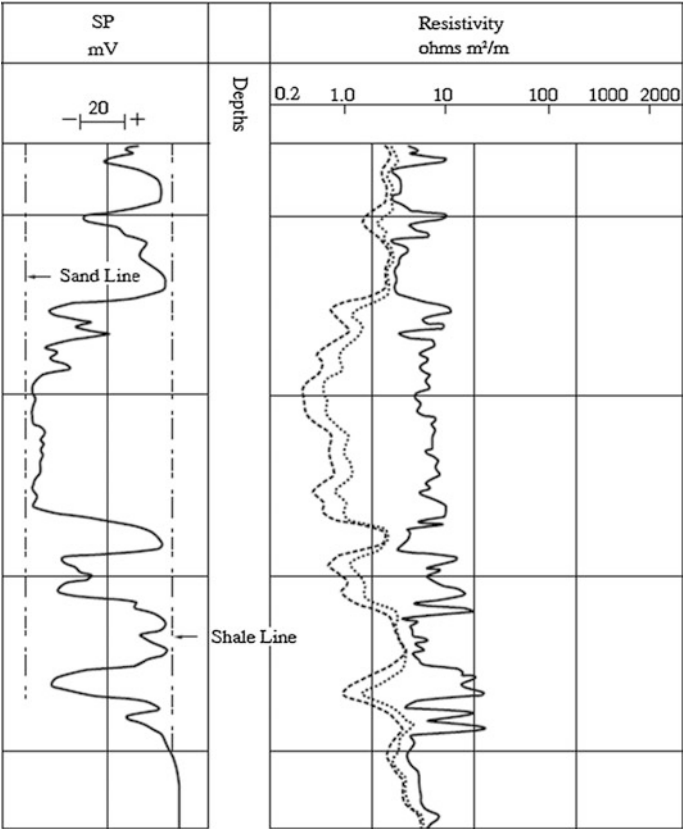


Fig. 2.8 Example of SP log in sand-shale sequence

2.2.4 R_w from the SP

If the permeable formation is not shaly, the total electrochemical force corresponding to the liquid junction and membrane potential, is equal to:

$$SP = K \log \frac{a_w}{a_{mf}} \quad (2.1)$$

Since chemical activities are of little value to the log analyst, Eq. 2.1 can be expressed in terms of water resistivity, which is also dependent on temperature.

Equation 2.2 solves for SP, given the resistivity of the formation water, the mud filtrate, and the formation temperature.

$$SP = -(60 + 0.133T) \log \frac{R_{mf}}{R_w} \quad (2.2)$$

where

$-(60 + 0.133T)$	the constant— K
T	the formation temperature in °F
R_{mf}	the resistivity of mud filtrate
R_w	the water resistivity

Equation 2.2 is the most popular form of the SP relationship. Note that an empirical relation has been substituted for the constant k , which enables its value to be calculated. Thus, if the total SP deflection can be found from the log and k can be calculated and R_{mf} can be measured from a flowline sample, the desired quantity R_w can be found.

2.2.5 Log Example of the SP

The measurement of the SP is probably the antithesis of the high-tech image of the logging techniques to be considered in subsequent sections. The sensor is simply an electrode which is referenced to ground at the surface, as shown in Fig. 2.9. The measurement is essentially a dc voltage measurement which is slowly time-varying as the passes in front of various formations.

To illustrate some of the characteristic behavior to be anticipated by the SP measurement on logs, refer to Fig. 2.10. In the left panel of this figure, a sequence of shale and clean sand beds is represented, along with the idealized respond. The shale base line is indicated, and deflections to the left correspond to increasingly negative values. In the first sand zone, there is no SP deflection since this case represents equal salinity in the formation water and in the mud filtrate. The next two zones show a development of the SP is largest for the largest contrast in mud filtrate and formation water resistivity. In the last zone, the deflection is seen to be to the

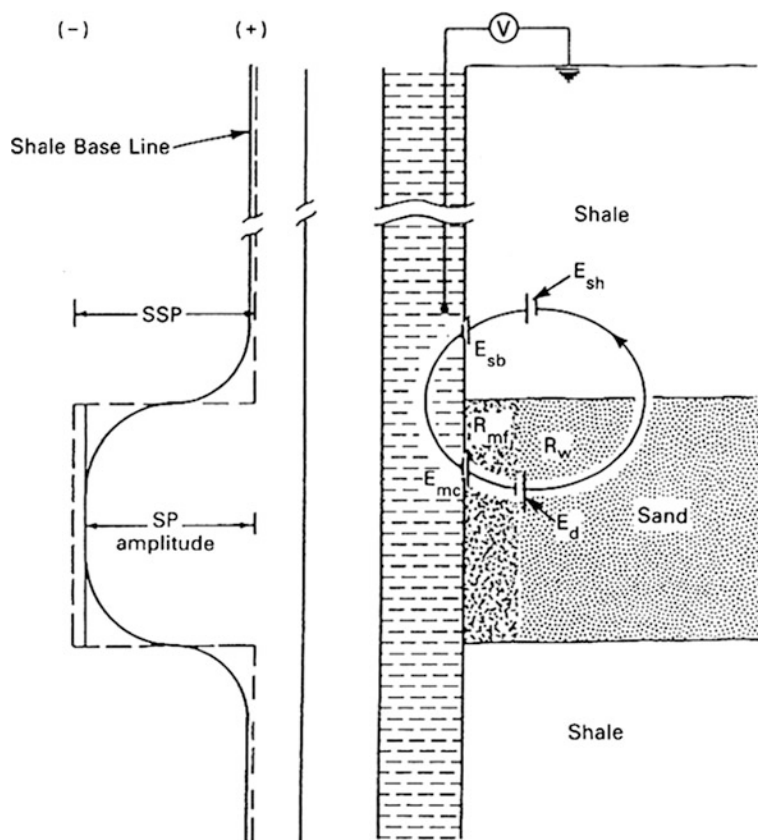


Fig. 2.9 A schematic representation of the development of the spontaneous potential in a borehole. Adapt from Dewan

right of the shale base line and corresponds to the case of a mud filtrate which is saltier than the original formation fluid.

The second panel of Fig. 2.10 illustrates several cases, for a given contrast in mud filtrate salinity and formation water salinity, where the SP deflection will not attain the full value seen in a thick, clean sand. (this latter value is referred to as the static SP, or SSP.) The first point is that the deflection will be reduced if the sand bed is not thick enough. Depending on invasion and the contrast between filtrate and water salinity, the bed thickness needs to be more than 20 times the borehole diameter to attain its full value. A second cause for reduced SP deflection is the presence of shale in rocks. In addition to these effects on the SP behavior, elaborate interpretations have been developed based on connections established between SP curve shapes and geological significant events. Some examples of using the SP curve to determine patterns of sedimentation are given in Reference 5.

Note that the SP builds up rather gradually from the base line and that the peak value is less than the SSP. This is referred to as the pseudostatic SP or PSP, and is

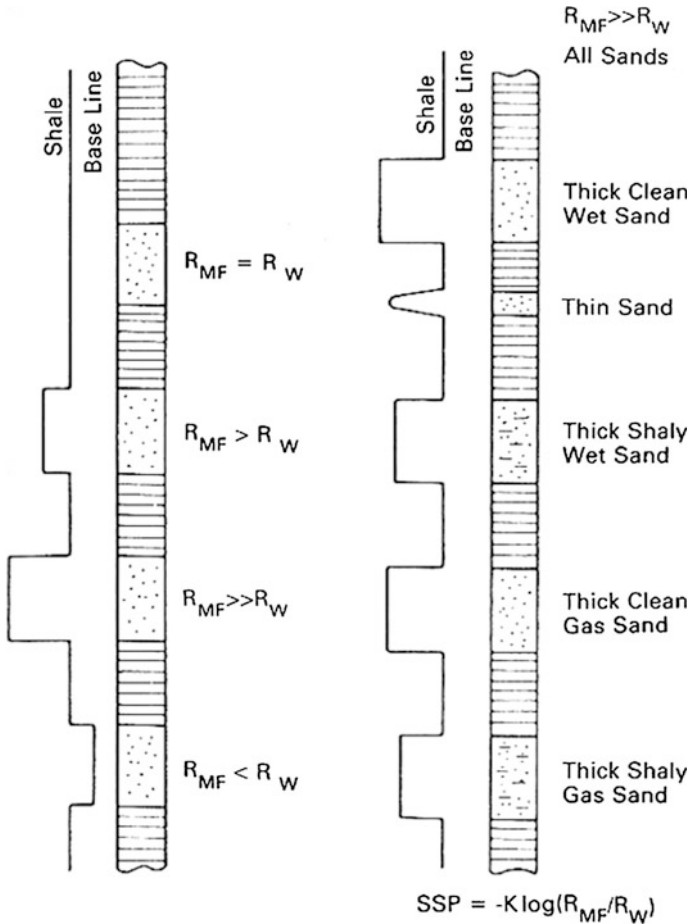


Fig. 2.10 Schematic summary SP curve behavior under a variety of different logging circumstances commonly encountered. From Asquith

strongly dependent on bed thickness, the resistivities of the invaded and virgin zones, depth of invasion, shaliness, and so on. These factors also affect the shape of the peak.

2.2.6 Applications of SP

In briefly, the applications of SP can be concluded as the followings:

- (a) Identification of porous, permeable beds.
- (b) Determination of R_W .

- (c) A lithological indicator: shales, coal-seams, shale fraction estimation from:
 $V_{sh} \leq 1 - \text{PSP/SSP}$.
- (d) An analysis of the facies and grading, based on the curve shape
- (e) Formation correlation.
- (f) An indication of possible hydrocarbon saturation in shaly sands, including the presence of a gas-oil contact.

2.3 Resistivity Logs

The measurement of formation resistivity is fundamental to the evaluation of hydrocarbon saturation. There are several measuring techniques in use, all variations of a common basic system: an emitter (electrode or coil) sends a signal (electrical current, electromagnetic field) into the formation. A receiver (electrode or coil) measures the response of the formation at a certain distance from the emitter.

Generally, an increase in the spacing of the system results in an improved depth of investigation (and a reading nearer to R_t), at the expense of vertical resolution.

Resistivity tools directly measure the effects of an electromagnetic field on the beds. Resistivity devices require a conductive fluid in the well bore to carry the current, whereas induction tools may be used in virtually any environment.

With any of these tools, different depths of investigation may be achieved by varying the spacings between signal source and sensor. Focusing coils or electrodes are often used to increase the effective depth of investigation and to improve bed boundary response.

A number of tools are of the resistivity type. Lateral log, Microlateral logs, Dual induction, 18" normal, 16" laterals, MicroSFL, and proximity tools are of this type. All of these are simply electrode arrangements.

Early resistivity logs, utilizing electrode-type devices, were called electric logs. Later, logs utilized a combination of induction and electrode devices and were known as induction-electric logs. An SP curve was commonly recorded in conjunction with both types of logs. Modern logs are merely developments of the induction-electric log.

No tool accurately measures resistivity of the intended zone, although some come very close. Between transmission and reception the signals transpire several distinctly different zones. Signals reaching virgin formation must cross the borehole fluid, the mud cake, the flushed zone, and the invaded zone. A portion of the total received signal will come from each of these zones. Corrections for such influences and for the influence of such factors as bed thickness must be applied to the values read from logs.

2.3.1 Normal Devices

The earliest electrical surveys used in well logging were the conventional resistivity logs with an SP. These devices consisted of electrode arrangements and some simple instrumentation. One such electrode arrangement is the short normal.

The short normal is a two-electrode measuring device which passes current from an electrode on the tool through the mud and into the formation. As depicted in Fig. 2.11. The Schlumberger short normal employs a 16" spacing. A deeper investigating design used 64" spacing. The deepest point at which the measurement is being made is midway between *A* and *M*. This point is considered the zero point for the device. The radius of investigation is very nearly equal to twice the electrode spacing. The mathematical relationship for this type electrode arrangement is depicted in the following:

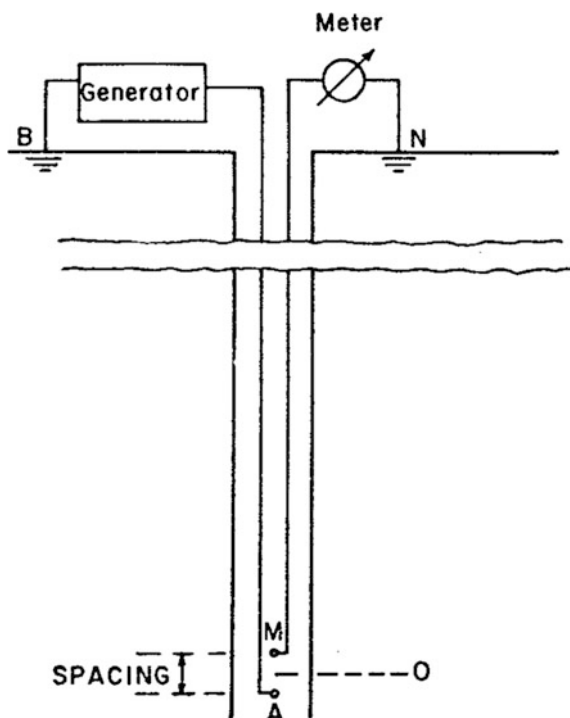
$$R = K \frac{V}{I}, \quad (2.3)$$

where

R resistivity, Ω m;

K constant

Fig. 2.11 Schematic of the normal resistivity tool



V voltage, V;

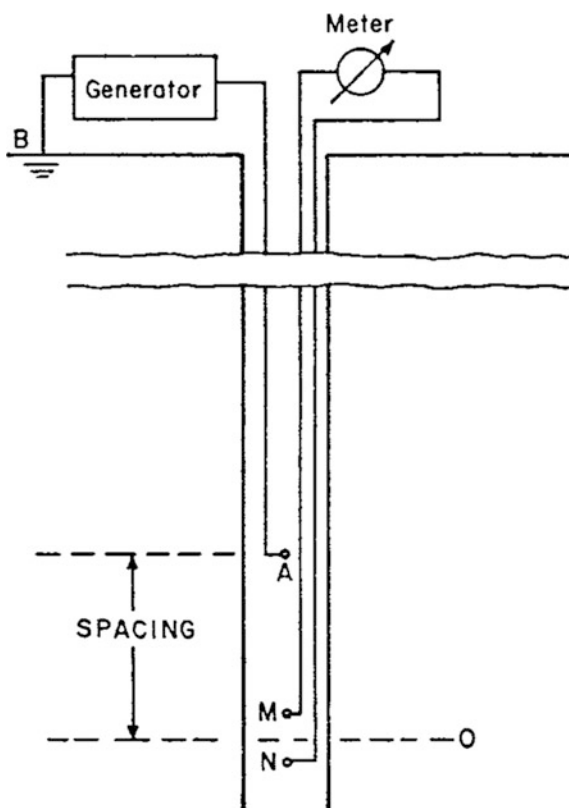
I current, A.

Resistivity is equal to K times voltage divided by current. The current, as previously stated, is constant. The proportionality constant K is related to electrode spacing and geometrical factors of the measuring device and formations. The only variable is the voltage. Log trace deflection, responding to voltage changes, can thus be scaled in resistivity units.

Looking at Fig. 2.12, we see a different electrode arrangement known as a lateral device. A constant current is passed between electrodes A and M and the potential difference is measured between electrodes M and N , which are located on two consequent spherical equipotential surfaces centered on A . The voltage measured is proportional to the potential gradient between M and N . The measuring or zero point for the device is at O , midway between M and N . Generally speaking, the spacing is approximately equal to the radius of investigation.

It is important to note that these devices record an apparent resistivity R_a . Resistivities will be affected by all the media surrounding the device, such as the borehole, the invaded and uncontaminated zones, and the adjacent beds. If quantitative R_t calculations are to be made, bed thickness must be 3–4 times the tool spacing.

Fig. 2.12 Schematic of the lateral tool (Courtesy of Schlumberger)



In today's logging industry, there are numerous devices available for the purpose of measuring the resistivity of the formation. Each device had a different depth of investigation. Accurate resistivity determination is necessary for the interpretation of hydrocarbons from a well. Each of the modern devices is designed to produce a good resistivity measurement for very specific ranges of borehole conditions. The first of these tailored tools we shall discuss is the focused-type devices.

2.3.2 Focused Tools

The influences of the borehole and adjacent formations on electrode devices are minimized by a family of focused current tools. The focused family of tools is designed for accurate R_t determination where R_t/R_m ratios are large, beds are resistive or thin, drilling muds are salty and conductive (where the ratio $R_{mf}/R_w < 4$), and large adjacent-bed resistivity contrasts.

Figure 2.13 shows a typical focused tool, with bucking electrodes A_1 and A_2 generating a current field (solid lines on a constant potential V_0) which focuses the current from the alpha ring (dotted lines). Alpha ring current penetrates deeply into the formation before the focusing fields become weak enough to allow it to disperse and return to the pickup electrode.

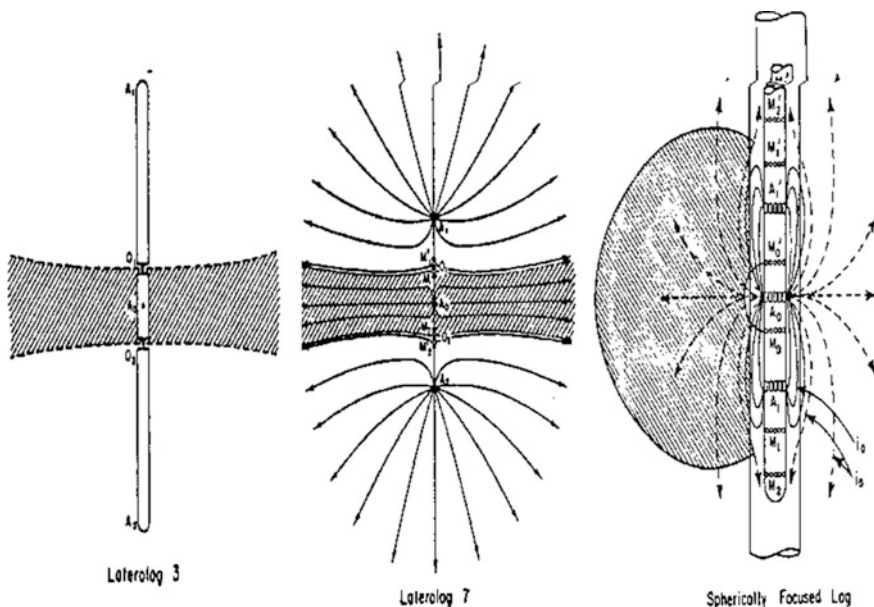


Fig. 2.13 Schematic of current flow of focused tool (Courtesy of Schlumberger)

Figure 2.14 shows an idealized focused log response. As you can see, it has reasonably good bed definition compared to normal electric logs. Also, the focused log gives us a much better definition of true resistivity. In this example, the shale resistivity is $5 \Omega\text{-m}$ and the resistivity of the sand is $250 \Omega\text{-m}$. Note that the mud is highly conductive, with a resistivity of $0.05 \Omega\text{-m}$.

2.3.2.1 Dual Lateral Log (DLL)

The objective of any deep-reading resistivity device is to measure the true formation resistivity, R_t . Deep-reading resistivity tools were designed so that, as much as possible, their response is determined by the resistivity of the virgin formation beyond the invaded zone. Unfortunately, no single measurement has yet succeeded in entirely eliminating the effects of the invaded zone.

This need, to detect deep, medium and shallow resistivity simultaneously, resulted in the development of the dual lateral logging (DLL) and micro-spherically focused logging tool with simultaneous recordings. DLL device is developed from LL3 and LL7, and combines features of them. Figure 2.15 is a sketch of the tool showing the electrode array used for the two laterolog devices. Both use the same electrodes and have the same current-beam thickness, but have different focusing to provide their different depth of investigation characteristics. Figure 2.16 illustrates

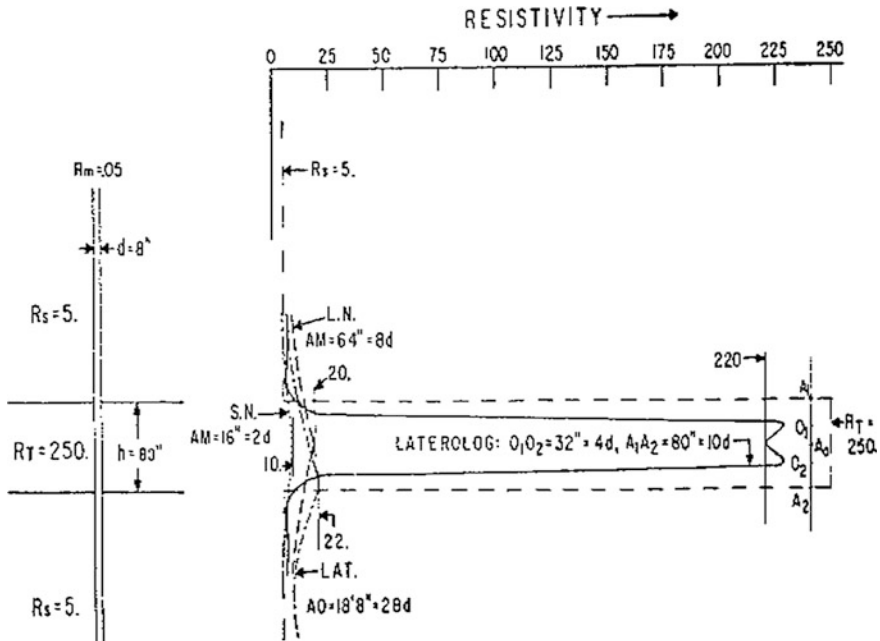
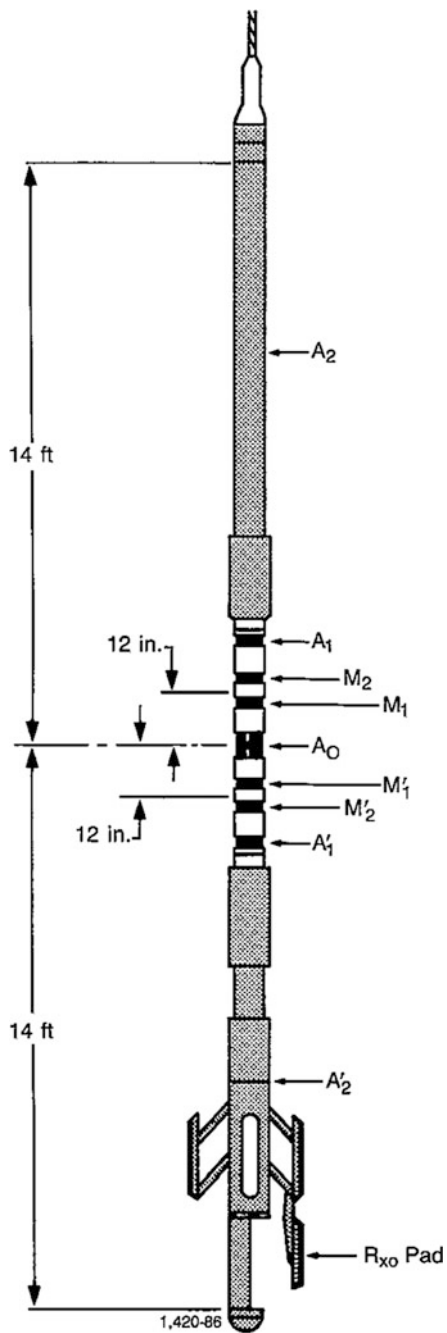


Fig. 2.14 Illustration of the focal curve response (Courtesy of Schlumberger)

Fig. 2.15 Schematic of
Laterolog and Micro-SFL tool
(Courtesy of Schlumberger)



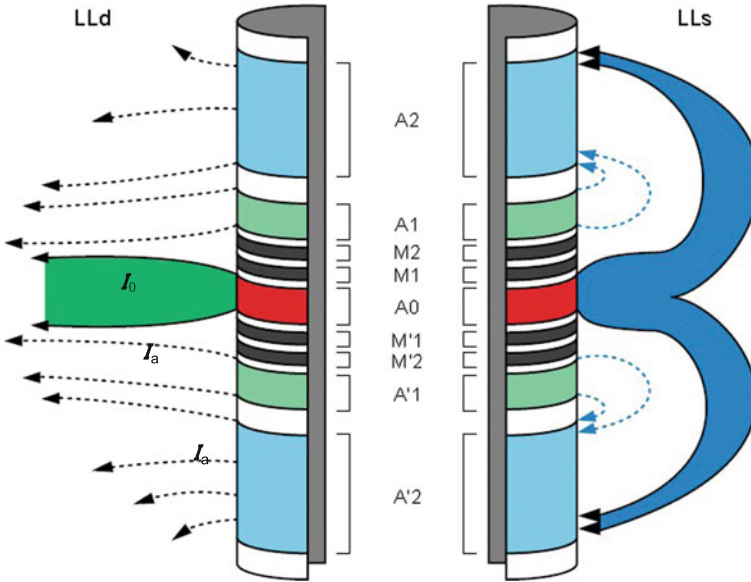


Fig. 2.16 Electrodes and current distribution of dual Laterolog tool

the focusing used by the deep laterolog device (left) and by the shallow laterolog device (right). The system is symmetrical above and below A_0 , the central electrode, which emits survey current I_0 . Electrodes M_1 and M_2 are shorted-circuited, as are M_1' to M_2' and A_1 to A_1' . The last pair inject an auxiliary or bucking current I_a of the same polarity as I_0 . A_1A_1' and A_2A_2' are two pairs of bucking electrodes, M_1M_1' and M_2M_2' , are two pairs of guard electrodes.

A control signal representing the potential difference between M_1M_2 and $M_1'M_2'$ is sent to the surface where it governs the current delivered to A_1A_2 . The system is self nulling in that the bulking current is continuously adjusted so as to maintain the condition $V(M_1M_2) - V(M_1'M_2') = 0$. Even when the mud column is taken into account, essentially no current from A_0 can flow vertically through the mud, and hence the central current I_0 was repelled into the formation. The potential measurement can be made at any of the M -electrodes. It converted to R_a through multiplied by a sonde coefficient K , which depends only on the distances between the electrodes (i.e., electrode spacing), as in the case of the normal and lateral sounds.

The DLL tool has a response range of 0.2–40,000 Ω -m, which is a much wider range than the previous laterolog devices, LL3, and LL7. To achieve accuracy at both high and low resistivities, a “constant-power” measuring system is employed. In this system, both measure current (I_o) and measure voltage (V_o) are varied and measured, but the product of the two (i.e., power), I_oV_o , is held constant.

The deep laterolog measurement (LLD) of the DLL tool has a deeper depth of investigation than previous laterolog tools, about 3.28 ft. To achieve this, very long

guard electrodes are needed; the distance between the extreme ends of the guard electrodes of the DLL- R_{xo} tool is approximately 28 ft. The nominal beam thickness of 2 ft, however, insures good vertical resolution.

The shallow laterolog measurement (LLS) has the same vertical resolution as the deep laterolog device (2 ft), but it responds more strongly to that region around the borehole normally affected by invasion. It uses a type of focusing called “pseudolaterolog,” where in the focusing current is returned to nearby electrodes instead of to a remote electrode, it has a relative shallow depth of investigation, about 2.46 ft.

2.3.2.2 Micro-SFL Logging (MSFL)

When the resistivity contrast between the invaded zone and the mud cake is high (i.e., high R_{xo}/R_{mc}), the current induced by the Microlog tends to escape through the mud cake (Fig. 2.17). To eliminate this problem, focused current-devices-Microlaterolog (MLL), the proximity log (PL) and the micro-spherically focused log (MSFL), were developed.

The MLL comprises one central electrode (A_0) and three ring electrodes (M_1 , M_2 , and A_1). These electrodes are imbedded in a pad, as shown in Fig. 2.18. The tool

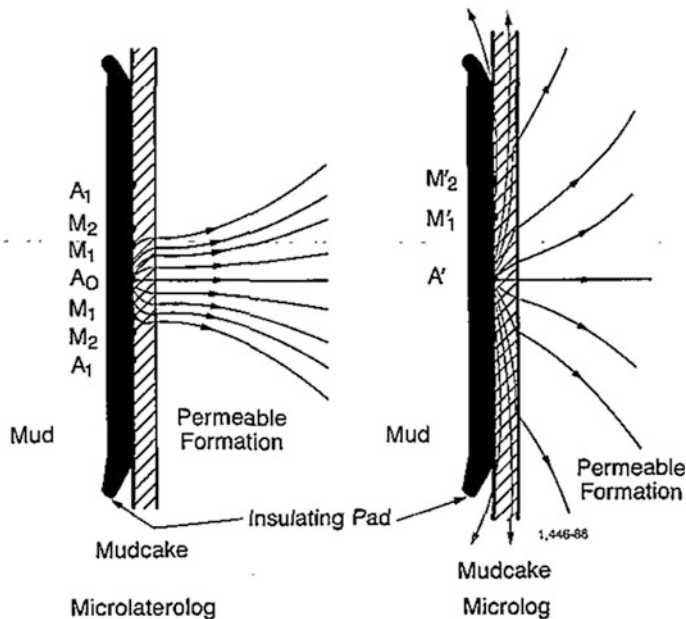


Fig. 2.17 ML current configuration of a permeable zone more resistive than the mud cake

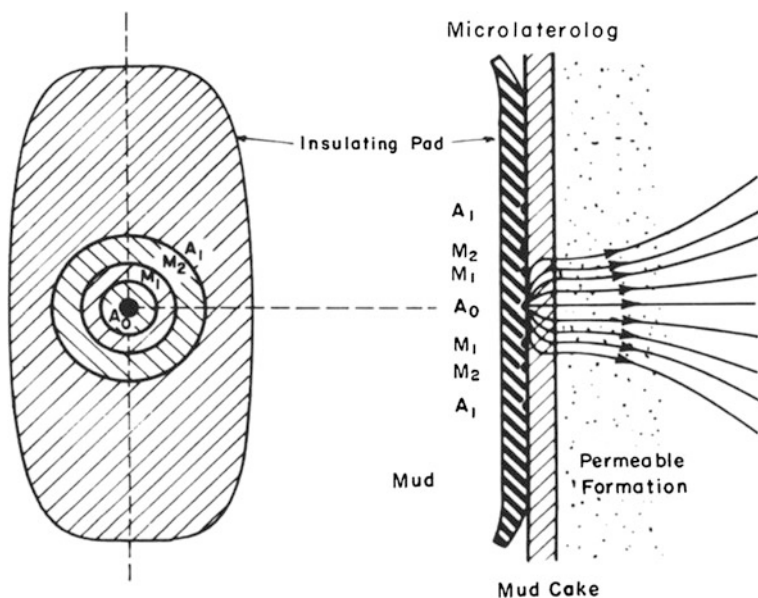


Fig. 2.18 MLL pad current distribution next to a permeable zone

functions identically to the LL7. When invasion is sufficiently deep and mud cake is $< 3/8$ in. thick, the MLL displays an apparent resistivity value that approximates R_{xo} .

The PL is similar in principle to the MLL. When a diameter of invasion equal to or greater than 40 in. is needed for the PL to provide direct approximation of R_{xo} , if the invasion is shallow, the reading is influenced by R_t .

The MicroSFL electrodes are smaller and pad-mounted. Figure 2.19 shows the electrode arrangement and current distribution of the MicroSFL. This design minimizes mud cake effect without requiring deep invasion, as with the PL. The MicroSFL provides good values of R_{xo} in a wider range of conditions than either the PL or MLL. Another distinct advantage of the MicroSFL is its compatibility with other logging tools, such as the Dual Laterolog and the induction SFL (Fig. 2.20). This eliminates the need for a separate logging run to obtain R_{xo} data. Figure 2.21 shows a log measured a log with DLL/MSFL combination tool. The MSFL, LLs, LLD are traced on the logarithmic scale in solid, dotted, and dashed lines, respectively. The thick formation located in the depth interval of 5687–5717 ft is characterized by a separation of the three curves. This separation indicates that the zone is invaded by mud filtrate; hence, it is permeable. This interval was drilled with saltwater-based mud ($R_{mf} = 0.056$ at 68 °F) that has a salinity exceeding that of formation water. The resistivity displayed by the logs increases with the tool's radius of investigation because of the salinity contrast between the mud filtrate and the formation water.

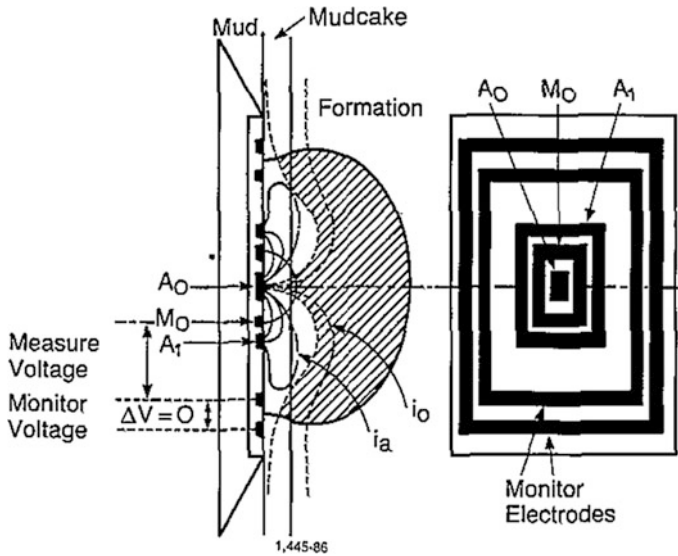


Fig. 2.19 Electrode arrangement and current distribution of Micro-SFL

2.3.3 Induction Tools

The induction log, introduced in the mid-1940s, was designed to measure formation resistivity in boreholes containing nonconductive fluids. Boreholes containing air, freshwater muds, or oil-based muds make excellent environments for induction logging. The induction log actually measures the conductivity of a formation rather than its resistivity. Conductivity is the reciprocal of resistivity, and vice versa.

Induction tools are focused to minimize the contribution of the borehole, invaded zone, and surrounding formation to the measurement. Focusing is realized by means of a system of several transmitter and receiver coils. The principle of the tool, however, can be simplified with the two-coil system in Fig. 2.22, which also shows the distribution of electromagnetic field. A transmitter coil is excited by an alternating current, $I(I_0 = \sin \omega t)$, of medium frequency (20 MHz). This current induces a primary alternating magnetic field, Φ , in the formation that surrounds the borehole can be referred a conductive ring. The magnitude and frequency of the field depends on the transmitter current. The vertical component of this induced magnetic field, in turn generates an alternating electric field e , which curls around the vertical axis. This electric field causes a rotational current, I' , to flow in the formation in circles concentric with the borehole. The rotational current, I' , is proportional to the electric field, and the formation conductivity, σ . the current that flows in a formation ring behaves as a transmitter coil and generates its own secondary magnetic field, Φ' . Φ' , which is proportional to the formation conductivity, induces an electric signal, V , in the receiver coil.

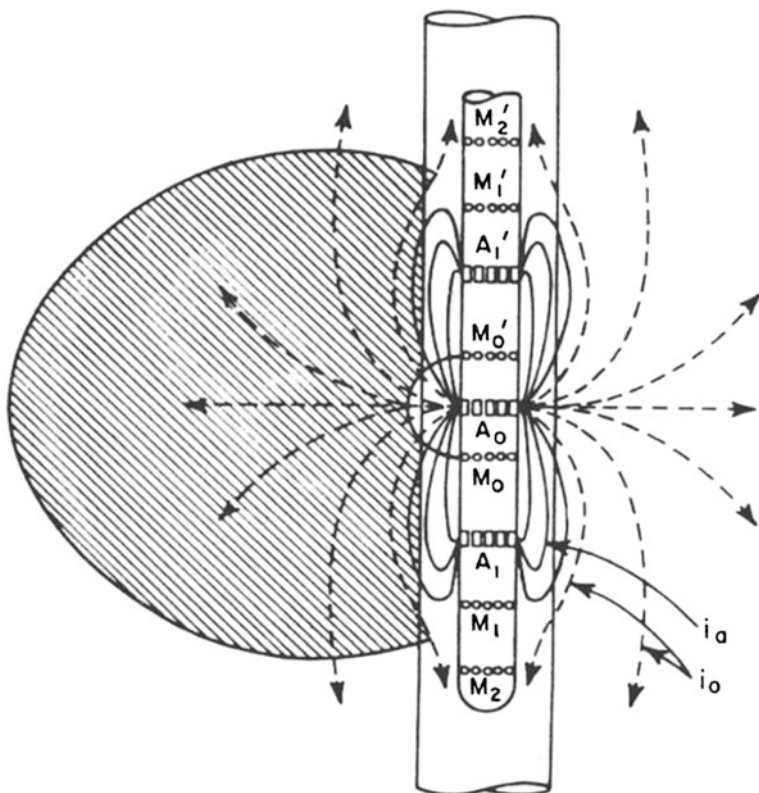


Fig. 2.20 Schematic of current pattern of the SFL

The primary and secondary alternating magnetic field will successively across the receivers, and inducing electromotive potential E_x and E_R . E_x is induced by Φ (hence by the current, I) directly coupling with receiver, and independent of conductivity of the formation, hence, it is called useless signal. E_R , however, is induced by Φ' (hence by the current, I') coupling with receiver, and dependent of conductivity of the formation, hence, it is called useful signal. By which, the electrical properties of the formation can be acquired. The process of electromagnetic field inducing is shown in Fig. 2.23.

Note that the phases of E_x and E_R are different, and the phase shift is 90° . E_R can be checked by a phase sensitive detector (PSD), and then the signal is converted to resistivity.

For an infinite homogeneous medium with conductivity σ , E_R is proportional to the σ , so:

$$E_R = K\sigma, \quad (2.4)$$

where, K is coefficient of induction tool.

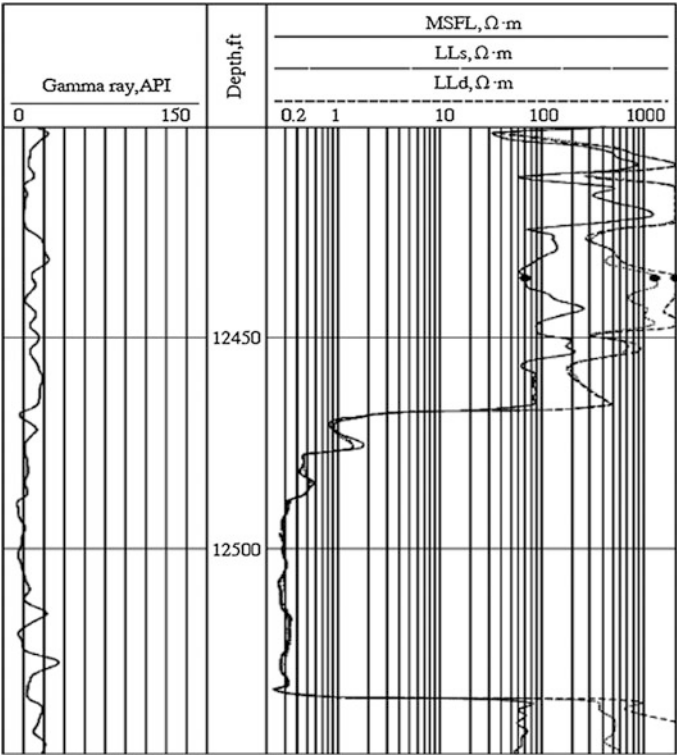


Fig. 2.21 Example of dual lateral log and MSFL log

Although dual induction tools were designed for a nonconductive borehole environment, they were found yield excellent measurement in water-based mud, provided that the mud is not too salty, the formation is not too resistive, and the borehole diameter is not too large.

A commonly used tool in oilfield is dual induction tool, which consists of a regular deep-induction device (ILD) and a medium-device (ILM). 0.8 m six-coil dual induction consists of three transmitter coils, T_0 , T_1 , T_2 and three receiver coils, R_0 , R_1 and R_2 . Among them T_0 and R_0 are central transmitter and central receiver coil respectively, and the distance between them is called main coil space. Auxiliary coil T_1 and R_1 are referred as borehole compensated coil, and T_2 and R_2 are shoulder compensated coil. Main parameters of these tools are the following, the number between two coils is the spacing of them (m), and the number in the next line is the turn number of corresponding coil, minus mean inverse direction with that of T_0 or R_0 :

Arrangement (m):	R_2 0.6	T_0 0.2	T_1 0.4	R_1 0.2	R_0 0.6	T_2
Turn number	-7	100	-25	-25	100	-7

(Negative signal means direction of coil, relative to the direction of central coils)

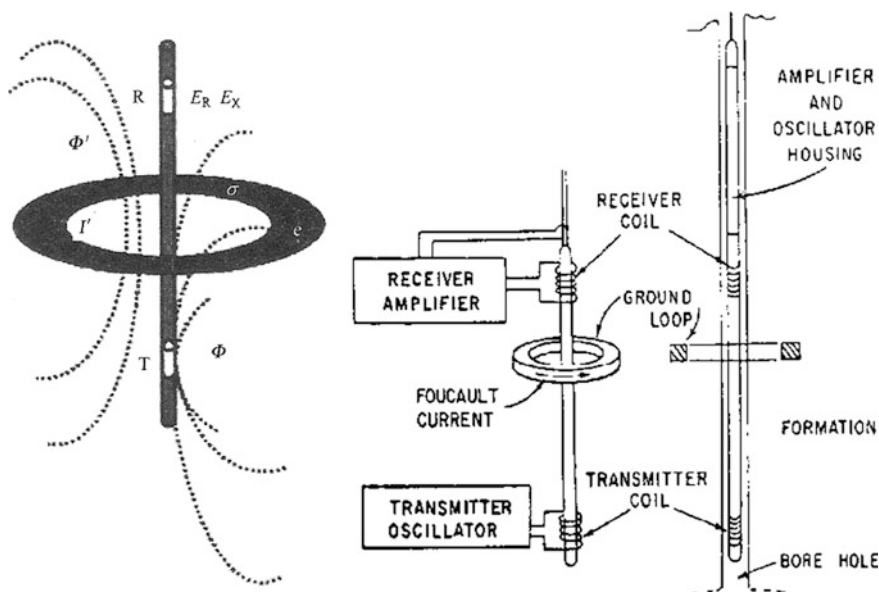


Fig. 2.22 Schematic of structure and electromagnetic field distribution of induction tool (Courtesy of Schlumberger)

Fig. 2.23 Inter-inducing process of electromagnetic field of DIL tool

$$I \rightarrow \Phi \begin{cases} \xrightarrow{90^\circ} E_X \\ \xrightarrow{90^\circ} e \rightarrow I' \rightarrow \Phi' \xrightarrow{90^\circ} E_R \end{cases}$$

Usually, the depth of investigation of ILD is 1.2–1.6 m and 0.65–0.8 m of ILM. The vertical resolution of ILD is about 2.5 m, and 1.8 m of ILM. The DIL curves are usually recorded with a shallow Laterolog, such as the LL8, or the SFL. Figure 2.24 shows a DIL/LL8 combination log. The practices show that this combination tool can acquire reliable measurements only if the $R_t < 100 \, \Omega \, \text{m}$, $R_{mf} < R_w$, and if diameter of borehole, $d_h < 8 \, \text{in. (20.3 m)}$ shallow or medium depth of invasion, and medium value of formation resistivity, this tool can still get relative reliable data.

Figure 2.25 illustrates an example of an induction log recorded in a borehole filled with an oil-based mud. The gamma ray log, discussed in Chap. 7, is recorded on the first track. The SP log usually displayed on the same track cannot be recorded in oil-based mud because it requires a conductive drilling fluid. The resistivity curve is shown on the second track. It is recorded on a linear scale, 0–10 $\Omega \, \text{m}$, increasing from EPT to right. The induction conductivity is shown on third track. It is recorded on a linear scale, 0–4000 $\text{m}\Omega/\text{m}$, increasing from right to EPT.

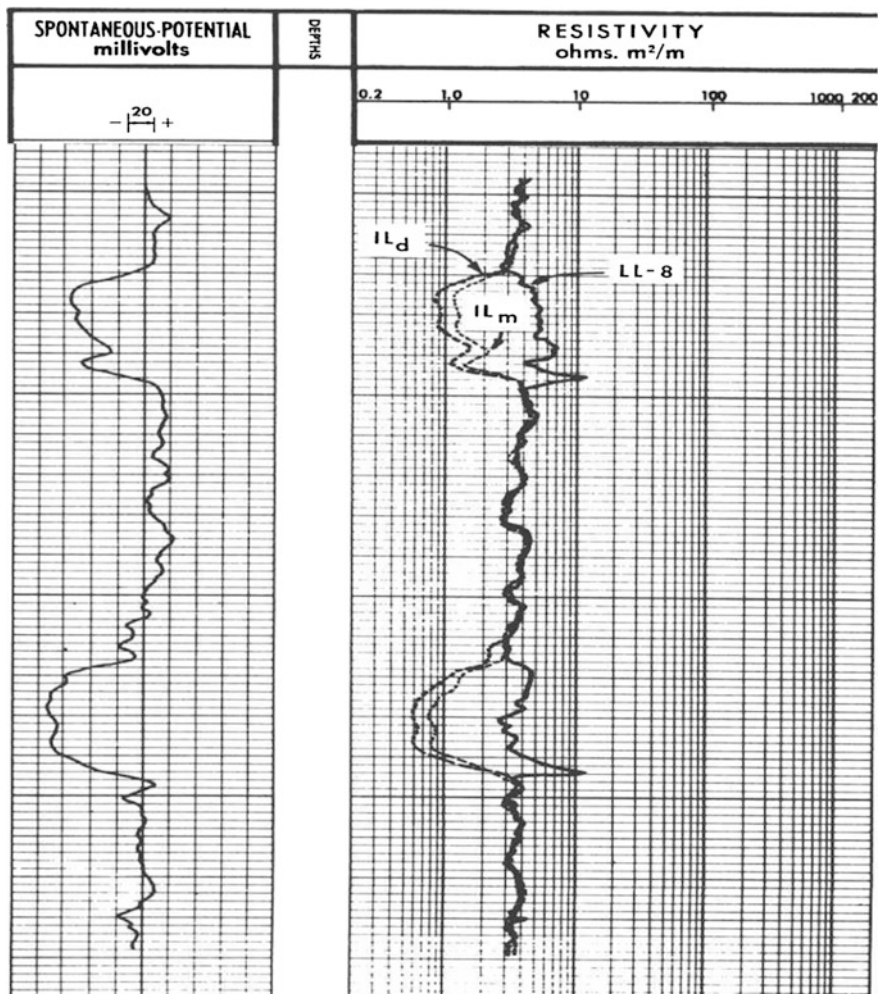


Fig. 2.24 Example of a dual induction/LL8

The scale are set up in this fashion so that the resistivity and conductivity curves move together in the same direction as the curve passes through zones of high and low resistivities.

Figure 2.26 shows a typical induction-electric log presentation. Direct output of the induction measuring circuitry is the conductivity curve in track 3. Corresponding resistivity is calculated automatically by an onboard computer, and output as the dotted induction resistivity curve in track 2. Off-scale resistivity values appear in track 2 at a different sensitivity. The solid curves in track 2 are resistivity from a shallow investigating electric device, in this case a 16" normal. Optimal conditions for running induction logs also produce excellent SPs.

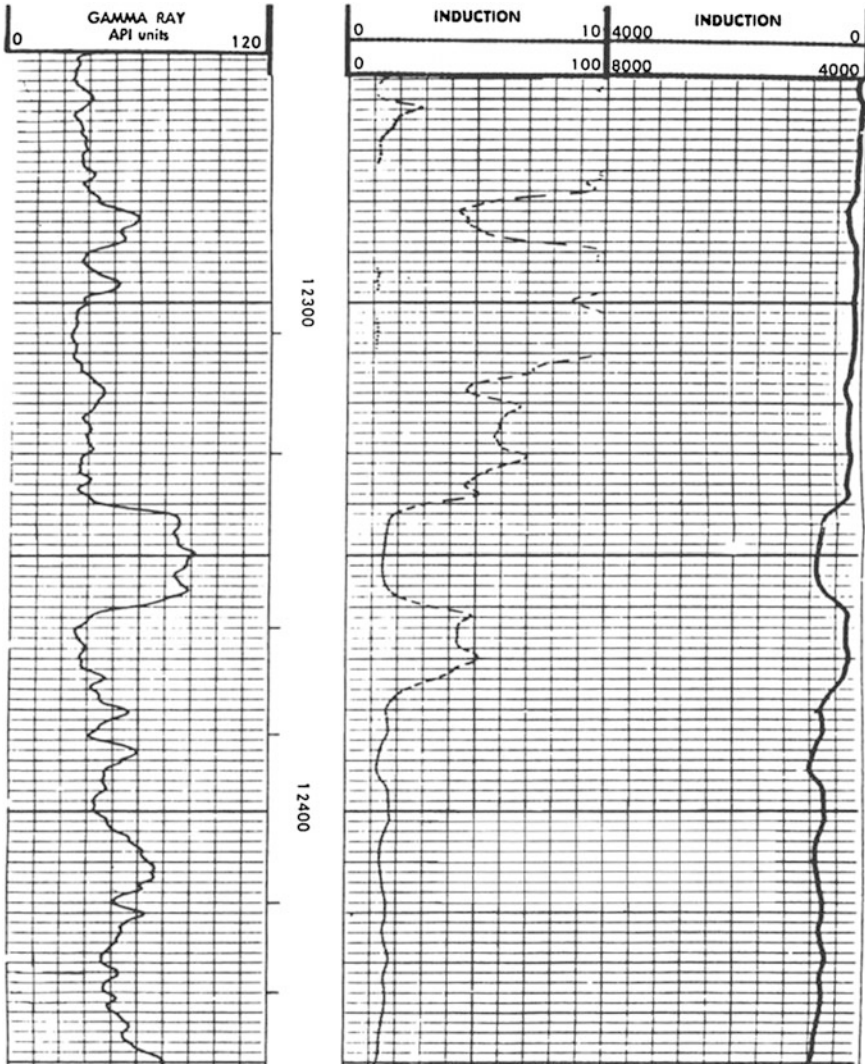


Fig. 2.25 Induction log record in a borehole filled with oil-based mud (Courtesy Amoco)

Under favorable logging conditions, the induction tool yields good values of true resistivities; however, charts may be needed where corrections can be found for bed thickness, large hole diameter, deep invasion, etc.

The dual induction tool is one of the most advanced resistivity devices available. It is particularly useful where invasion diameters are large. An SP and/or gamma ray curve is also recorded with it. The dual induction tool records three resistivity curves having three different depths of investigation. A shallow curve measures the flushed zone resistivity. A medium curve measures invaded zone resistivity. A deep

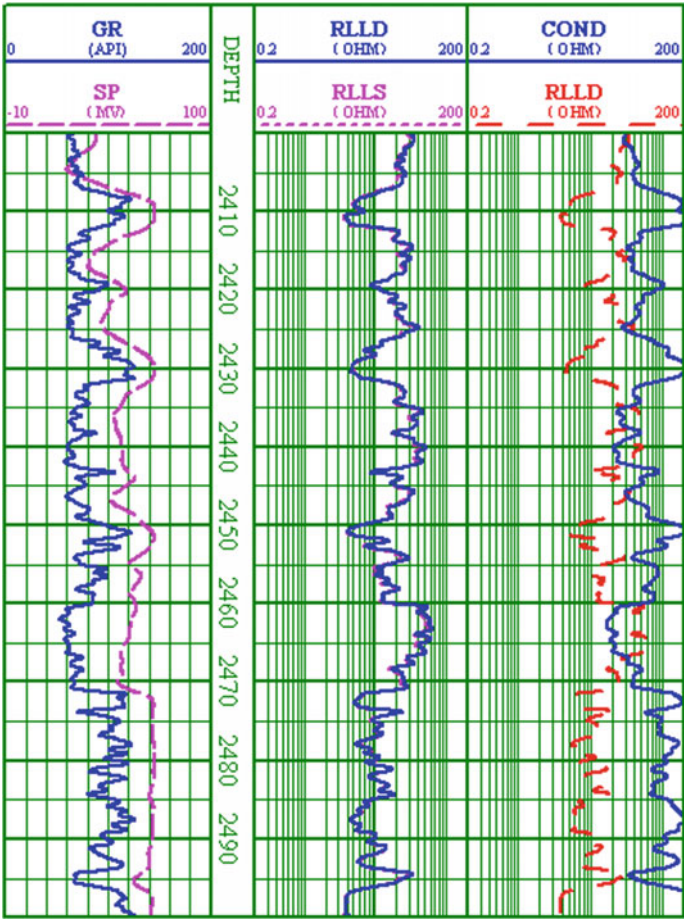


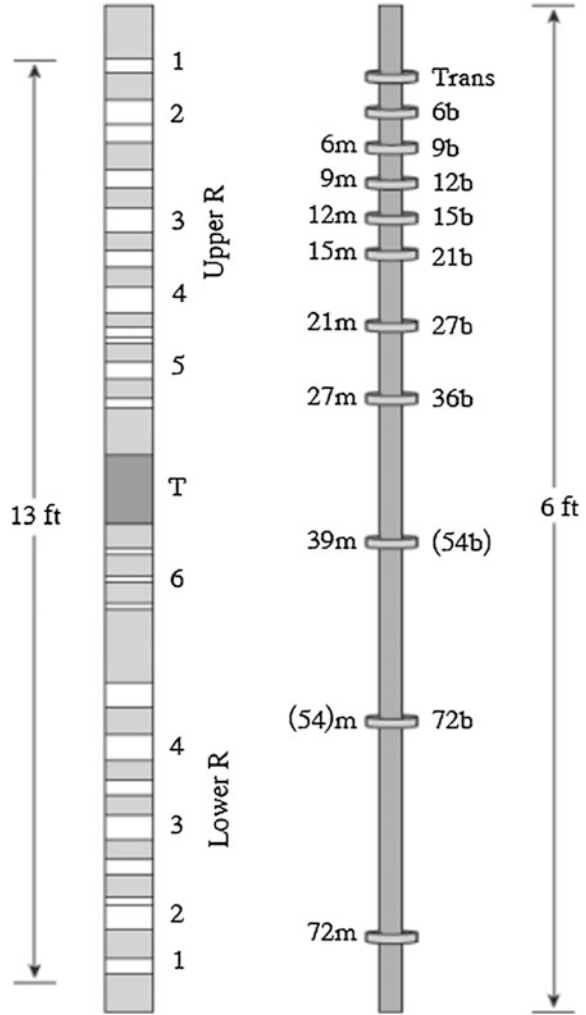
Fig. 2.26 Illustration of the conductivity and resistivity curves

curve measures primarily the uncontaminated or virgin zone and is very close to R_t . The ratios of shallow to deep and medium to deep are used to determine R_w , R_t and the diameter of invasion, d_i .

2.3.4 Array Induction Tools (AIT)

The Array Induction Imager Tools (AIT, Fig. 2.27) accurately measure open borehole formation conductivity as a function of both well depth and radius into the formation at different borehole conditions and environments. Various tools cater to special operating environments, including slim wells and hostile, high-pressure,

Fig. 2.27 Coil layout for the high-resolution array induction tool



high-temperature (HPHT) environments. Wireline array induction tools use an array induction coil that operates at multiple frequencies. The distance between central coils of AIT tool ranges from several inches to dozens inches, for example, 6", 9", 12", 16", 21", 27", 39", and 72". The AIT tool has three operation frequencies, 25, 50, and 100 kHz; and it can provide three different vertical resolutions, 1', 2' and 4', five different radial investigations with 10", 20", 30", 60", and 90".

The Applications of AIT can be summarized as the following:

- Reservoir delineation
- Determination of true formation resistivity R_t
- Determination of S_w

- Hydrocarbon identification and imaging
- Determination of movable hydrocarbons
- Invasion profiling
- Thin-bed analysis

2.3.5 FMI (*Full Borehole Microresistivity Image Logging*)

Since the mid-1980 there has been an explosive development imaging technology, principally in terms of tools but also in terms of producing the image. The progress has been linked with availability of downhole digitization of signals and the possibility of transmitting large data volumes in real time. Where the standard logs are sampled every 15 cm(6"), image logs may sampled every 0.25 cm(0.1"); where the standard logs have one measurement per depth point, image logs may have 250, the region of 200 kbits per second transmitted up the cable to achieve a collection rate of 60,000 samples per meter of borehole. Imaging technology is still evolving rapidly and is affecting the entire logging field. Table 2.2 lists typical image tools of some international oil field service company.

Coils 1 are two identical 3-coil arrays equidistant either side of T. Coils 2–6 are 4-coil arrays. Not all bucking coils are shown. (From Beste et al.) (Right) Coil layout for the AIT-H tool. m are the main coils and b the bucking coils. In most cases the bucking coils are co-wound with the main coils of the next smallest array. The spacings of the main receivers increase approximately exponentially from 6 in. Coil spacings are given in inches.

In the mid-1980s, Schlumberger introduced their first electrical imaging tool, the Formation MicroScanner (FMS), as an evolution of their SHDT dipmeter. The first tools only provide as image of 20 % of an 8.5" borehole, using just two pads. Since

Table 2.2 Imaging tools of different company

Company	Symbol	Name	Description
Schlumberger	FMI	Fullbore Formation MicroImager (current tool 1996)	4pads + flaps 192(4 × 48)electrodes
Schlumberger	FMS	Formation MicroScanner (older tool 1pre-1991)	2 or 4 pads 54(2 × 27)electrodes 64(4 × 16)electrodes
Halliburton	EMI	Electrical MicroImager	6 independent pads 150(6 × 25)electrodes
Western Atlas	*STAR	Simultaneous Acoustic and Resistivity (Borehole image)	6 independent pads 150(6 × 25)electrodes

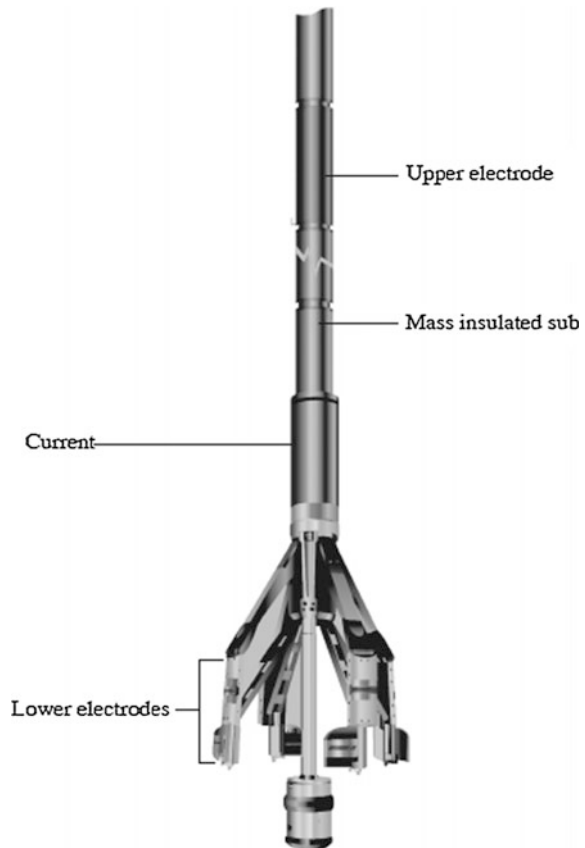
then there has been steady progress in borehole coverage. The present tool, the Fullbore MicroImager provide nearly 80 % coverage in an 8.5" borehole of high quality images.

FMI consists of four arms, the adjacent two arms are orthogonal and each arm has two pads (Fig. 2.28), the each pad has a hinged flap. Both pad and flap have arrays of 24 electrodes.

The FMI provides an electrical borehole image generated from up to 192 microresistivity measurements. Applications of FMI are listed below:

- Structural geology
- Structural dips, even in fractured and conglomeratic formations; detection and determination of faults.
- Sedimentary features
- Determination of sedimentary dips and paleocurrent directions
- Definition and characterization of sedimentary bodies and their boundaries
- Recognition of anisotropy, permeability barriers, and permeability paths
- Recognition and evaluation of thinly bedded reservoirs

Fig. 2.28 Schematic of the configuration of FMI tool



- Rock texture
- Qualitative vertical grain-size profile; Determination of carbonate texture
- Detection and evaluation of secondary porosity
- Detection and evaluation of fracture systems
- Complement to coring and formation tester programs
- Depth matching and orientation for whole cores.

Figure 2.29 shows that FMI provided image of different formation conditions, for (a), carbonate zone with fracture on the wall of well, because of the mud invasion into the fracture, the resistivity decreased, and then a relative dark block corresponding to the fracture depth. (b) also shows features of fracture formation, nearly parallel to each other of the waves implying fracture occurring in the formation. The dark color in image (c) indicates shale or clay zone with resistivity. Nonuniform distributed dark color spots in the image (d) shows that a lot of caves and vugs existed on the sidewall of well.

2.3.6 ARI (*Azimuthal Resistivity Imager*)

The ARI azimuthal resistivity imager makes directional deep measurements around the borehole with a higher vertical resolution than previously possible from conventional laterolog tools. Using 12 azimuthal electrodes incorporated in a dual laterolog array (as shown in Fig. 2.30), the ARI tool provides a dozen deep-oriented resistivity measurements while retaining the standard deep and shallow readings. A very shallow auxiliary measurement provides data to fully correct the azimuthal resistivities for borehole effects.

The ARI tool is combinable with a wide variety of other tools and is particularly effective for thin-bed evaluations in combination with the IPL integrated porosity lithology tool string.

ARI images also complement images from the UBI ultrasonic borehole imager or the FMI full borehole formation microimager because of the tool's sensitivity to features beyond the borehole wall and its lower sensitivity to shallow features.

Table 2.3 Properties of FMI tool

Tool	No. of electrodes	Hole diameter (%)			Logging speed
		6"	8 ^{1/2} "	12 ^{1/4} "	
FMI	4 pad + flaps 192	90	80	50	1800'/h
FMI	4 pad 96	50	40	25	3600'/h
FMI	4 pad 64	50	40	25	1600'/h
FMI	2 pad 54	25	20	12	1600'/h
SHDT	(8)				5400'/h

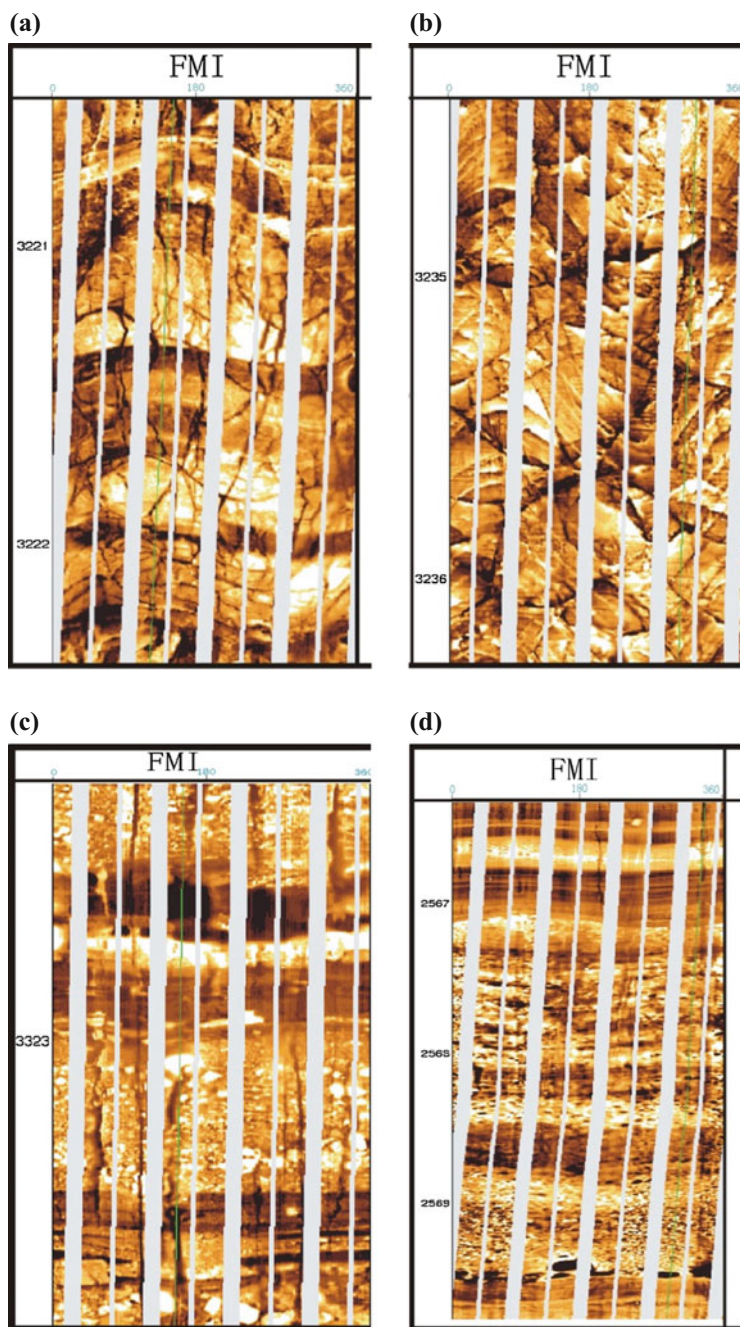


Fig. 2.29 FMI image for different formations. **a** FMI image of formation, **b** FMI image of fracture formation, **c** FMI image low resistivity shale zone, **d** FMI image of pores and caves

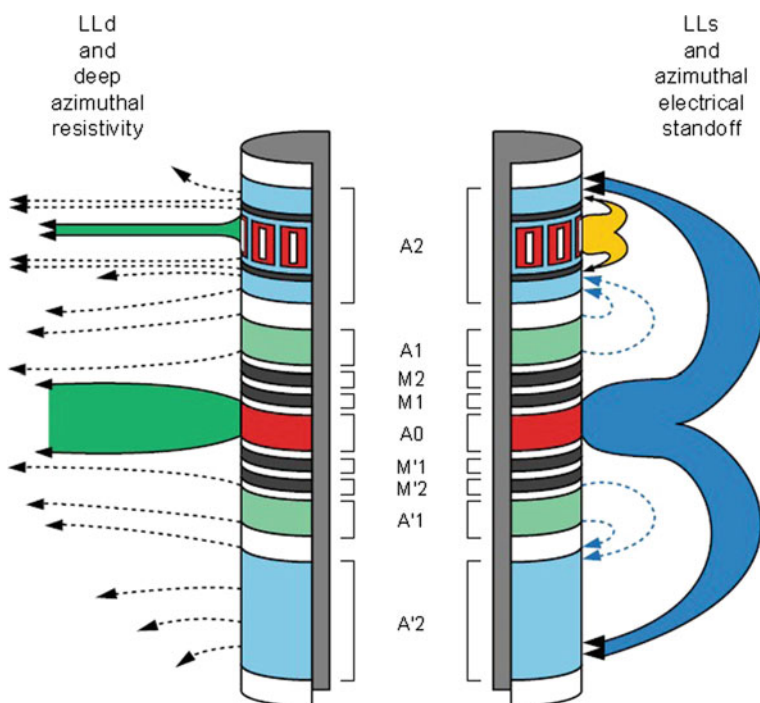


Fig. 2.30 Configuration of ARI tool

Applications of ARI

Resistivity logs and images with vertical resolution of less than 1 ft

Thin-bed analysis

Fracture identification and characterization

Evaluation in deviated and horizontal wells

Evaluation of heterogeneous reservoirs.

2.4 Dipmeter Logging

The aim of this log is to determine the angle to the horizontal and the azimuth referenced to magnetic north and geographical north of the dip of the planes cut by the well. These planes can be: bed boundaries; an open or closed fracture; an erosional surface; a stylolitic joint.

The planes can be planar, or can correspond to a convex or concave surface intersecting the well.

2.4.1 Principle

A plane is defined by a minimum of three points not lying in a straight line. It should be sufficient, therefore, to know the coordinates (X , Y , Z) of three points in space to define the plane. These three points will be the intersection of three generatrices of the borehole wall with the plane (Fig. 2.31).

2.4.2 Measurement Process

The tool consists of at least three electrodes mounted on pads in a plane perpendicular to the axis of the tool and situated at angles of 120° (3-pad tool) or 90° (4-pad tool) to each other, the configuration of this tool is shown in Fig. 2.32.

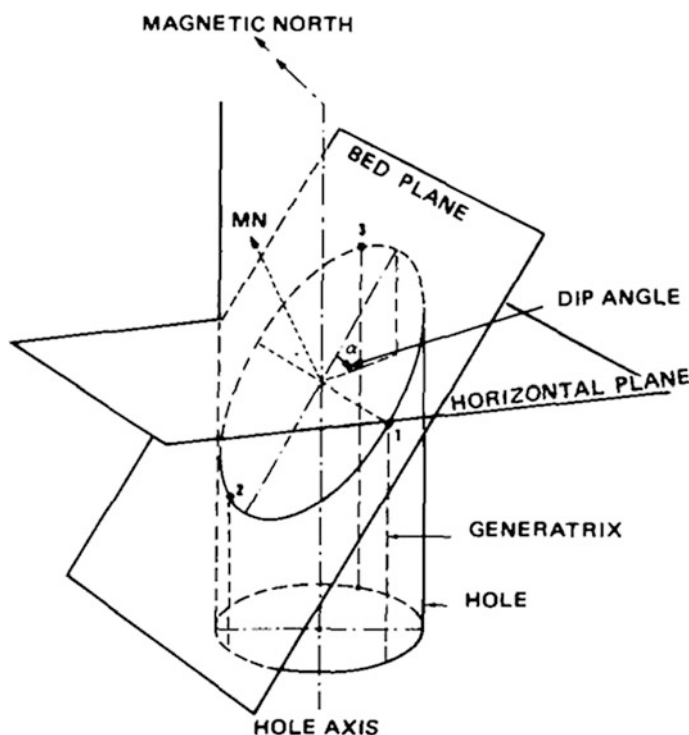


Fig. 2.31 A plane is defined by a minimum of three points not lying on a straight line. The three points are the intersection of three generatrices of the borehole wall with the plane (i.e., bed boundary)

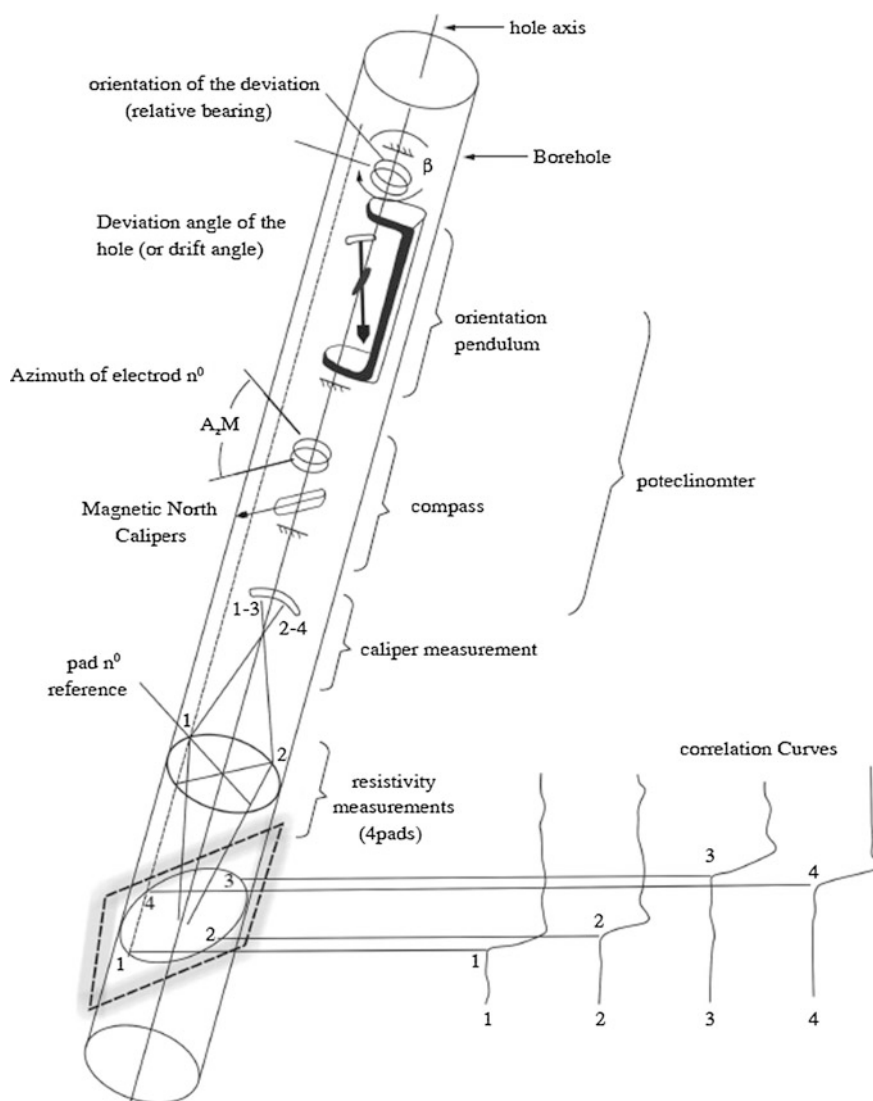


Fig. 2.32 Principle of the dipmeter showing the different measurements made by the tool (from Dresser-Atlas document)

The three electrodes each make a resistivity measurement of the borehole wall. Because of the size of the electrode and the current focusing that occurs on each pad the resistivity measurement is assumed to be a point measurement at the electrode. When the tool crosses the boundary between two formations the corresponding response change is recorded for each pad at different depths according to the

apparent dip (that is to say in relation to the borehole axis). The relative depth differences for the curves give the necessary information to evaluate the dip and the azimuth if we also know:

- (a) the orientation of the sonde defined by the azimuth and one of the pads (pad number 1). This azimuth is the angle formed by the horizontal projection of the lines perpendicular to the sonde axis and passing through pad number 1 and magnetic north;
- (b) the borehole deviation and its azimuth;
- (c) the hole diameter (or more exactly the distance between the sonde and each pad).

The azimuth of pad 1 with respect to magnetic north is measured using a compass to which is fixed the cursor of a potentiometer. The movement of the compass pointer is reflected in changes in the potentiometer resistance. The borehole deviation is measured using a pendulum linked to a potentiometer whose resistance varies as a function of the deviation. The azimuth of the deviation is measured by means of another pendulum that is continuously aligned in a vertical plane passing through the low side of the borehole. This pendulum is linked to a circular potentiometer whose resistance is a function of the angle formed by the azimuth of the deviation and of the azimuth of pad number 1 as reference (called the relative bearing). Finally the hole diameter is measured using potentiometers linked to the sideways movement of the pads.

2.4.3 *SHDT*

The Schlumberger SHDT (Sedimentary Dipmeter Tool) dipmeter, for example, with four independent arms, each carrying a pad with two small circular electrodes side by side and 3 cm apart. The sampling is made every 1/10 in. (2.5 mm). This system acquires more information on sedimentary structures: lithological or textural changes over very short distances can be detected. In addition the tool deviation is more precisely measured by a new magnetometer. The tool also has an accelerometer which allows better speed corrections, resulting in a more accurate dip measurement. The Emex current is automatically adjusted to always have the highest contrast in resistivity.

A typical dipmeter field log will show not only the raw microresistivity curves, but also most of the orientation and caliper data. The example chosen is from a western Atlas, 4-arm(pad) Diplog (Fig. 2.33). In track 1 are the deviation of the borehole from the vertical (DEV) and azimuth (DAZ), the azimuth (AZ) of the reference pad (pad1) and a gamma ray. In track 2 and 3 are the raw acquisition curve, the tension and the two calipers. The tension curve is useful in identifying zones of tool sticking although these are usually evident on the caliper and the raw

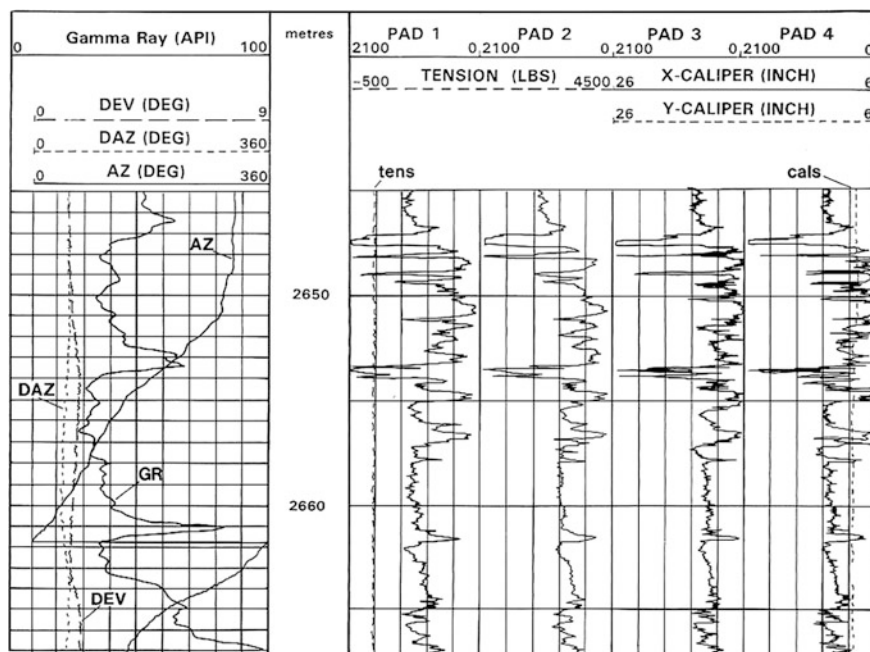


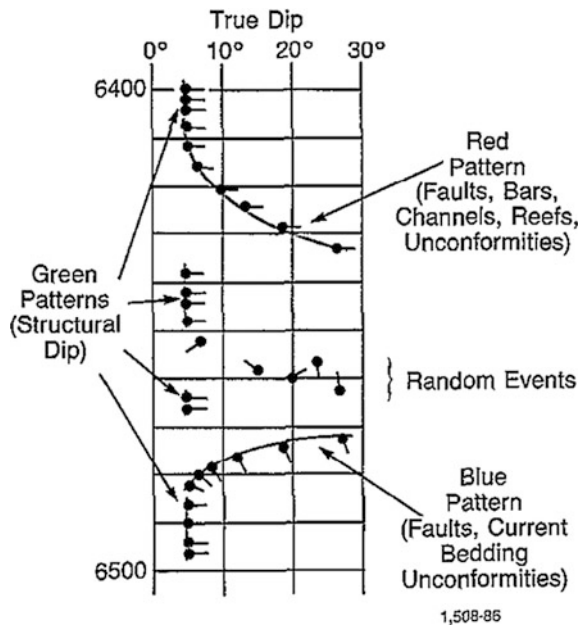
Fig. 2.33 Standard log presentation of raw dipmeter data. The dipmeter curves are sampled every 0.5 cm (0.2") while the standard logs are sampled every 15 cm (6") (western Atlas Dip log). *DEV* Hole deviation from the vertical. *DAZ* Azimuth of hole deviation. *AZ* Azimuth of pad 1. *pad 1-4* Pad conductivity curves

curves themselves. The format of the raw dipmeter data varies between companies although the basic information included is similar. The log is plotted at a 1:200 scale.

2.4.4 Colored Dip Patterns

More than 20 years ago, the pioneers of log-derived dip interpretation devised a color-coding scheme for different computed dip patterns. Structural dip is usually colored green on computed dip arrow plots, a method to identify graphically those intervals having consistent magnitude and direction of dip. The color is, of course, arbitrary, but the color-coding scheme has evolved into an acceptable industry standard. For studies of sedimentary dip, it was found useful to sort out the apparent confusion of dip arrows with different colored lines joining groups of dip arrows that fit different dip patterns and/or directions. The color scheme, as shown in Fig. 2.34, is that which is generally accepted in the industry today.

Fig. 2.34 Four colored dip patterns for common formation structure



2.4.4.1 Red Pattern

Red dip patterns connect those dips that increase in magnitude with increasing depth, the azimuth remaining roughly constant. Red dip patterns are usually associated with such geological features as:

- faults and folds,
- unconformities,
- differential compaction (e.g., above reefs, bars, domes, etc.),
- within channels, troughs, and valley fills.

2.4.4.2 Blue Pattern

Blue dip patterns connect dips that decrease in magnitude with increasing depth, with the azimuth remaining roughly constant. Blue dip patterns are usually associated with features such as:

- faults or folds,
- unconformities,
- paleocurrent features.

Blue dip patterns associated with paleocurrent features are usually found over short depth intervals, while blue dip patterns associated with faults, folds and unconformities might persist over much longer depth intervals.

2.4.4.3 Green Pattern

Green dip patterns are usually found in shales. However, shale do not always exhibit such coherent dip because of slumping, fracturing, diapirism, etc. conversely, a green dip pattern does not always represent post-depositional structure. Parallel crossed-bedding will also reflect consistent dip azimuth. Low structural dip ($<5^\circ$) is the most difficult to identify because dip azimuth is often widely scattered. If the scatter is restricted to low dip magnitudes, structural dip is essentially flat, with no preferred direction indicated. For more than a 2° dip magnitude, the average direction can usually be determined by auxiliary plots.

2.4.4.4 Random Pattern

Random events correspond to a chaos of dip and azimuthal, which are changed irregular with increasing depth. Random dip pattern are usually associated with fault and fracture zone caused by tectonic movements.

2.4.5 Results Presentation

The results of computer processing of data recorded in a well are presented in various forms.

(1) Listing presentations

The Service Company gives dip computation results in the form of listings.

In the case of MARK IV the listings given by Schlumberger give the following data in 13 columns: Depth; Dip angle; Dip azimuth; Deviation angle; Caliper 1-3 diameter; Caliper 2-4 diameter; LOG1 corresponding to the program logic (Table 2.4).

(2) Graphical presentation

Dip results may be presented graphically in many ways.

1. Arrow plots (Fig. 2.35)

This is the most widely known presentation, and can be produced at depth scales of 1/1000, 1/500, or 1/200. Each calculated point is plotted:

- (a) In abscissa according to the dip angle.
- (b) In ordinate with depth.

The point is extended by a short straight line in the dip direction, with geographical north towards the top of the plot (or log). Also shown are: (a) the angle

Table 2.4 Normal listing of MARK IV (Courtesy of Schlumberger)

Depth (m)	DIP (°)	DIP AZM(°)	DEV (°)	DIAM1-3 (in.)	DIAM2-4 (in.)	PLA (°)	CLO (°)
952.4	15	94	1.2	12.5	12.3	11	100
953.3	14.3	108	1.4	12.5	12.4	85	53
954.3	10.2	158	1.3	12.4	12.4	0	100
955.3	36.7	221	1.4	12.6	12.5	0	0
956.3	10.6	352	1.4	12.6	13.4	0	100
957.3	24.3	288	1.4	13.6	13.4	0	51
958.3	23.7	102	1.5	14.2	13.4	0	100
959.3	37.2	181	1.6	13.3	12.9	0	100
960.3	26	170	1.6	13.2	13	0	95
961.3	19.9	149	1.6	13.3	13	0	16
962.3	13.9	144	1.5	12.5	12.4	0	100
963.3	41.2	268	1.4	12.3	12.4	0	100

and azimuth of the borehole deviation (intervals of 50 m or 100 ft, usually); and (b) a scaleless resistivity curve allowing depth correlation with other logs. This curve is drawn with low resistivities to the EPT.

Different symbols are used to represent points:

- (a) A black circle indicates a good quality result.
- (b) An open or white circle indicates a point for which the quality is undefined
- (c) A cross shows that the four-pad logic has been used, however, this symbol is not used in the standard presentation.

2.4.6 Stick Plot

A stick plot represents dip as a line. Because no azimuth can be indicated, stick plots are usually presented in two (sometimes more) sections, one at 90° to the other: typically a north-south and an east-west set. The sticks represent the apparent dip in the orientation indicated (Fig. 2.36). The plots are most effective using broad interval averages and small vertical scales to illustrate an entire well. Figure 2.36 shows a standard dipmeter tadpole plot with corresponding dip azimuth against depth plot (center) and two, orthogonal orientations of stick plot (right). The azimuth plot is especially useful in structural analysis. The stick plot is used on correlation cross-sections and for seismic comparisons. Stick plot can be useful added to correlation diagrams.

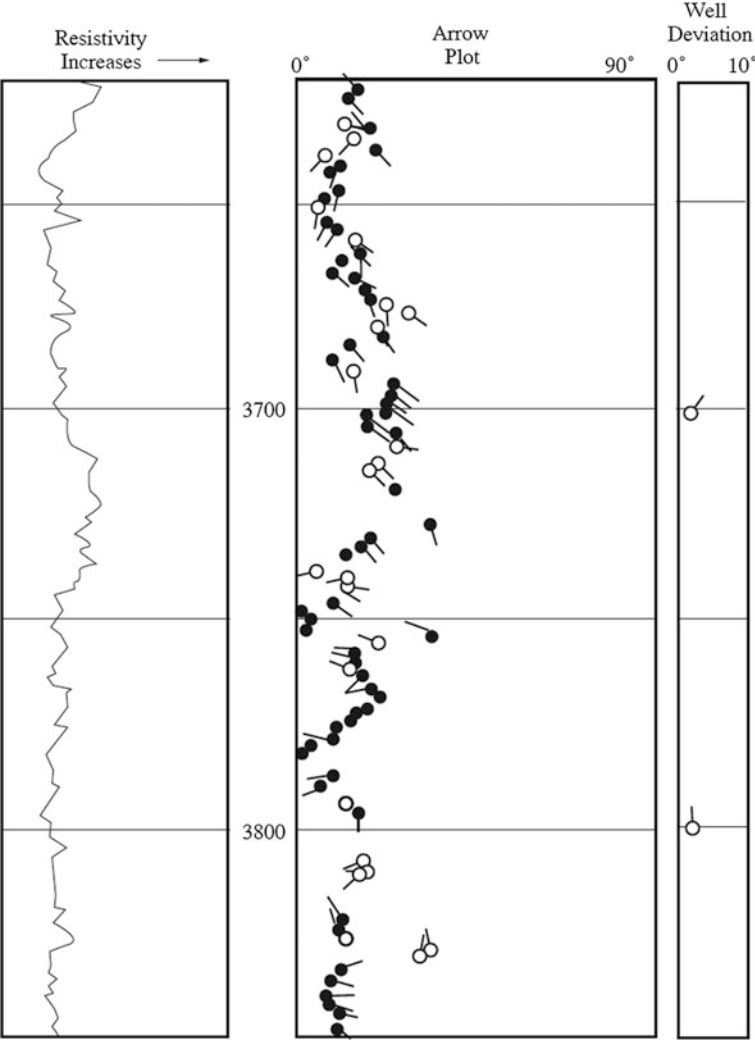


Fig. 2.35 Example of arrow plots

2.4.7 Azimuth Frequency Plots

Calculated azimuth values in a depth interval are plotted in the form of circular histogram (Fig. 2.37). The value of the azimuth is read clockwise from 0° to 360° and the frequency of occurrence is shown as a radial line whose length is proportional to the number of points whose azimuth falls in the range. Zero values are at the center.

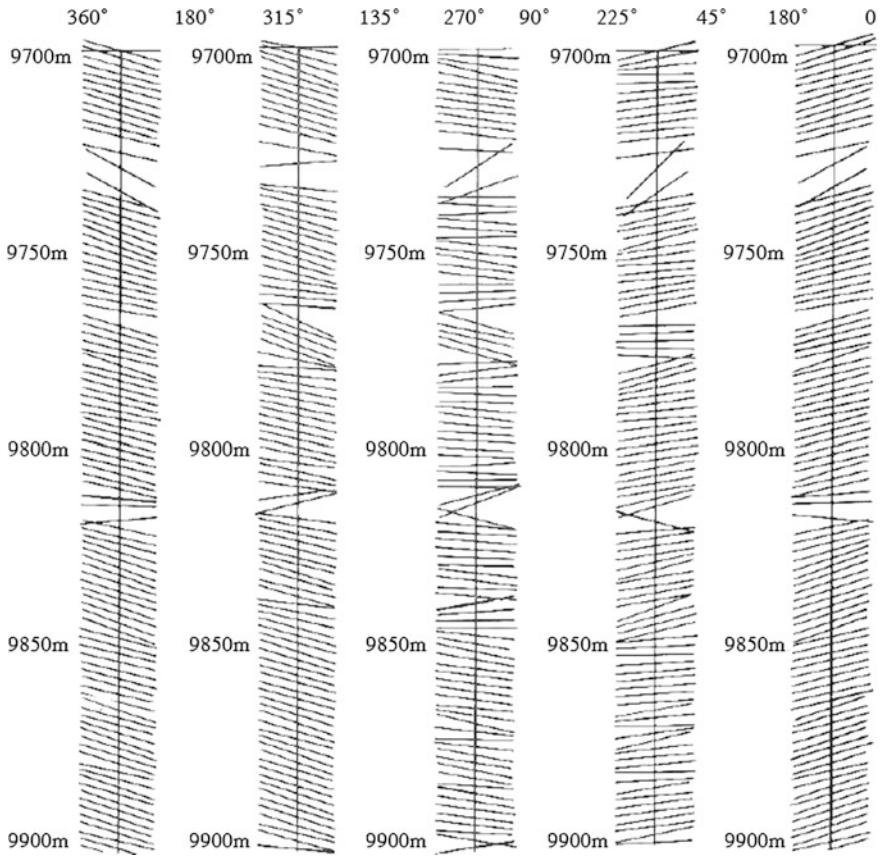


Fig. 2.36 Standard tadpole and stick plot

The plots allow the determination of azimuth trends, the azimuth or regional dip, sedimentary dip. The plots are also widely used to identify geological structure, sedimentary environments, fracture zone, fault, unconformity. Meanwhile, the caliper, azimuth and dip curves can be applied to determine the stress, stability of wall.

2.5 Summary

Resistivity devices display apparent resistivity values, R_a . The apparent resistivity, R_a , measure at a depth of interest is affected by the resistivity geometry of four zones that surround the tool: the borehole, adjacent beds, and the invaded and uninvaded zones of the bed of interest. The apparent resistivity value should be corrected for the borehole and the adjacent-bed (also called bed thickness) effects. The corrected value R_a'' , bears the influence of the invaded and uninvaded zones.

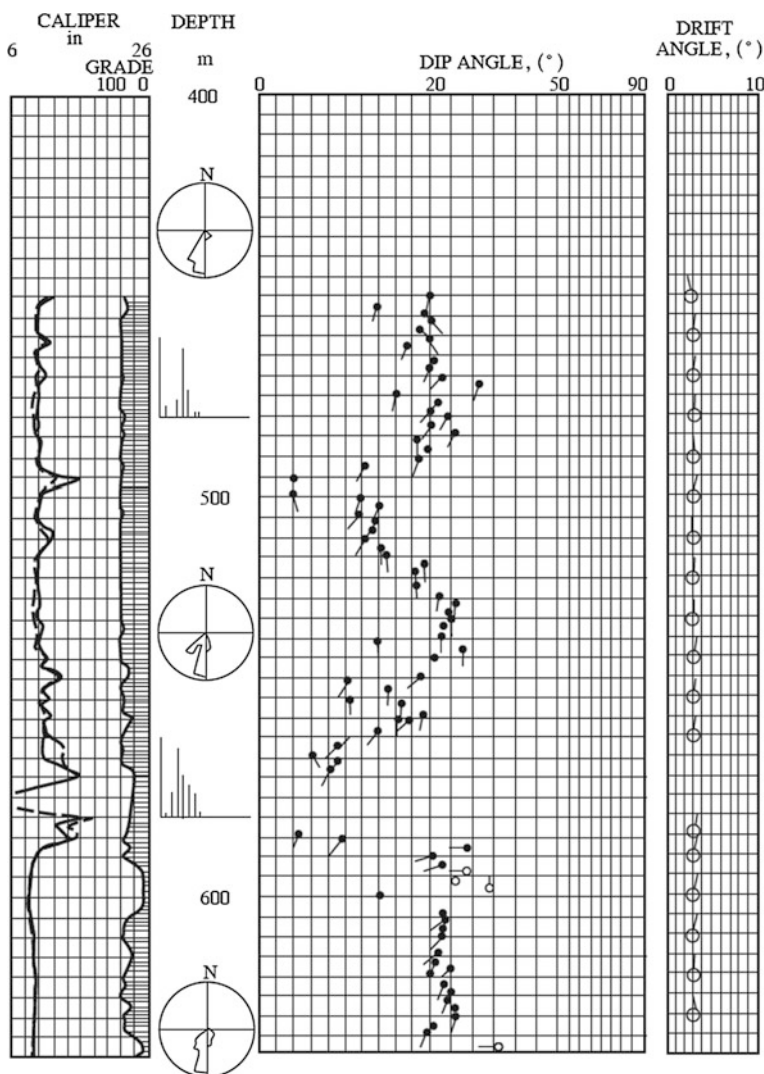


Fig. 2.37 Azimuth frequency plot

Depending on the type and number of resistivity logs available, R_a'' is used to calculate R_t , R_{xo} , or both. Departure curves (charts) are usually used to perform these corrections and calculations.

Determining R_t and R_{xo} requires three steps.

The apparent resistivity R_a , is first corrected for borehole effects by use of R_m and dh . Correction of readings of microresistivity devices requires R_{mc} and h_{mc} instead. For each resistivity tool, optimum measurement conditions exists in which the borehole effect is nil or negligible.

The value obtained from Step 1, R_a' , is then corrected for bed thickness effect with the resistivity of the adjacent bed R_s , and the thickness of the bed in question. No adjacent-bed corrections are necessary when the bed thickness exceeds a certain value. This value depends on the tool's vertical resolution and the resistivity contrast R_t/R_s . Reading of microresistivity tools are free from this effect.

The last step is to use the value R_a'' obtained in Step 2 to calculate R_t and R_{xo} . The calculation calls on the geometric factors. Departure curves or a system of equations is used. If the diameter of invasion is small, the effecting invasion is negligible and $R_t = R_a''$. On the other hand, for microresistivity devices, when invasion is deep, the effect of the uninvaded zone becomes negligible and $R_{xo} = R_a''$.

In certain measurement environments, the three effects (borehole, bed thickness and invasion) are negligible. In these cases, R_t or R_{xo} can be read directly from the log.

In some instances, the data available lead to unrealistic results, such as negative values, or the data fall off the tornado chart. In the most instances, such an occurrence is the result of values improperly read or improperly corrected for borehole or bed thickness effects. However, in cases of very deep invasion with an invasion profile that cannot be approximated by a step profile, such a case may result. Treatment of other invasion profiles, such as the transition and annulus profiles, requires extensive data; four resistivity readings are usually needed.

Problems

- 2.1 What are the characteristics of resistivity of rocks?
- 2.2 Draw a sketch of the environments of borehole in view of resistivity
- 2.3 Describe the Archie's experiment and the formulas to calculate S_w .
- 2.4 Explain the mechanism of the occurrence of SP
- 2.5 What are the properties of SP and its applications?
- 2.6 What is the principle of focused resistivity logging?
- 2.7 Describe the configuration of DLL tool.
- 2.8 Explain the measurement principle of DLL method.
- 2.9 What are the characteristics of DLL curve?
- 2.10 How to determine the fluid type of the formation by using DLL curves?
- 2.11 Explain the principle of DIL method
- 2.12 What is the characteristics of DIL curve?
- 2.13 How to determine the fluid type of the formation by using DIL curves?
- 2.14 What is the advantages of image resistivity logging?
- 2.15 What 'is the configuration and applications of AIT?
- 2.16 What is the configuration and applications of FMI?
- 2.17 What is the principle of dipmeter logging?
- 2.18 What is dip pattern of dipmeter logging presentation?
- 2.19 Explain the characteristics of the four dip patterns respectively?

<http://www.springer.com/978-3-662-54976-6>

Principles and Applications of Well Logging

Liu, H.

2017, XIV, 356 p. 217 illus., 48 illus. in color., Hardcover

ISBN: 978-3-662-54976-6